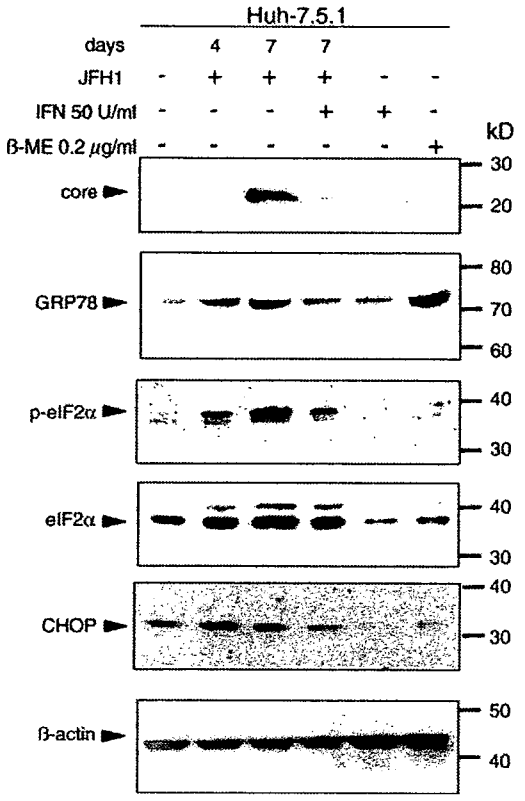

Fig. 5. Expression of ER stress-related proteins in HCV-JFH1 infected cells. The supernatant of JFH1-transfected Huh-7.5.1 cells was transferred onto uninfected Huh-7.5.1 cells. The cells were harvested at 4 and 7 days after infection. The JFH1-infected cells were also cultured with interferon (50 U/ml) or 2-mercaptoethanol (0.2 μg/ml) and harvested after 48 h after treatment. 2-Mercaptoethanol was used as a positive control to induce ER stress (Nakagawa et al., 2005). Western blotting was performed using anti-core, anti-GRP78, anti-phospho-eIF2-alpha (p-eIF2α), anti-eIF2-alpha, anti-GADD153/CHOP, and anti-beta-actin antibodies. β-ME, 2-mercaptoethanol.

level of CHOP expression was apparently increased in JFH1-infected Huh-7.5.1 cells.

To determine whether ER stress contributes to the formation of cytopathic plaques, JFH1-infected cells were incubated in methylcellulose-containing medium and double immunofluorescence staining of the plaques was performed. As shown in Fig. 6, overexpression of GRP78 was colocalized with HCV-core-positive cells with and without CPE. Together with the result shown in Fig. 4, these findings suggest that ER stress is induced in the HCV-JFH1-infected cells and these responses may be involved in development of apoptosis and the formation of cytopathic plaques.

A cytopathic clone could be isolated and this had acquired a high infection efficiency and increased cytopathogenicity

The plaque assay enabled differential quantification of viral infectivity and cytopathogenicity by the immunofluorescence detection of HCV core protein in JFH1-infected, plaque-developed cultures. The number of plaques, as well as infectious foci, was linearly proportional to the dilution of an inoculum (Fig. 7B). It was revealed that only a few populations of HCV-positive foci developed cytopathic plaques (Fig. 3B and Table 1). The infectious focus-forming units and plaque-forming units were 5.6×10^3 FFU/ml and 9.7×10^2 PFU/ml, respectively (Table 1).

To determine whether the difference between the cytopathic and noncytopathic HCV-JFH1 replication might be attributable to viral factors, we isolated clones from each cytopathic plaque. JFH1-infected Huh-7.5.1 cells were incubated in DMEM containing methylcellulose. Cytopathic plaques became visible at ~1 week after inoculation. We isolated cells from each plaque using a cloning cylinder, subcultured, and transferred supernatant onto uninfected Huh-7.5.1 cells. To our surprise, infection of naive cells with plaque-derived supernatants led to massive cell death at 10 days post-infection (Fig. 8A). The supernatant of these cells was transferred again onto uninfected Huh-7.5.1 cells again. Immunofluorescence assay revealed that almost 100% of the cells were positive for HCV core protein (Fig. 8B). The infectivity and cytopathogenicity of this isolated plaque (Pl #1) were 4.9×10^3 FFU/ml and 3.0×10^3 PFU/ml respectively (Table 1), much higher than the parental JFH1 clone. Moreover, the ratio of PFU to FFU in a plaque-isolated clone (Pl #1) was significantly higher than that of parental JFH1 clone (0.58 and 0.17 respectively) (Table 1 and Figs. 7B and C). We next performed an infection experiment of the parental JFH1 and a plaque-derived clone by adjusting infectious titers of the inocula by HCV core antigen levels. As shown in Fig. 8C, virus from cytopathic plaque (Pl #1, #2, #3) showed significantly higher elevation of core antigen levels in supernatants than the parental JFH1 in every time point. The second round isolation of plaques from the Pl #1 subclone (Pl #1-1, #1-2 and #1-3 in the Table 3) showed consistently higher replication efficiency and cytopathogenicity. These results indicated that JFH1 subclones isolated from cytopathic plaques showed significantly higher infection efficiency and greater cytopathic effects than the original JFH1.

The isolated plaque had amino acid substitutions clustered in the NS5B region

To determine whether there are viral mutations in the cytopathic JFH1 subclone (Pl #1), we performed sequence analyses. As shown in Table 2, 11 nucleotide changes were found in the cytopathic plaque, and 9 of these were non-synonymous mutations (81.8%). In particular, 6 of the 11 mutations (9153, 9232, 9293, 9295, 9353, and 9355) were clustered in the C terminal half of the NS5B region. We also performed sequence analyses of the Pl #1-isolated subclones, Pl #1-1, #1-2, and #1-3, and other clones that had been independently isolated from different plaques, Pl #2, #3, and #4 (Table 3). Those subclones showed similar mutations within NS5B region. The C2438S, P2934S, and S3001N substitutions were redundantly appeared in the 4 plaque-isolated clones and in all three Pl #1-derived subclones. In contrast, no mutations were found in the virus from infectious foci without plaque formation. These results showed an evidence that certain amino acid mutations were directly associated with the viral replication efficiency and cytopathogenicity.

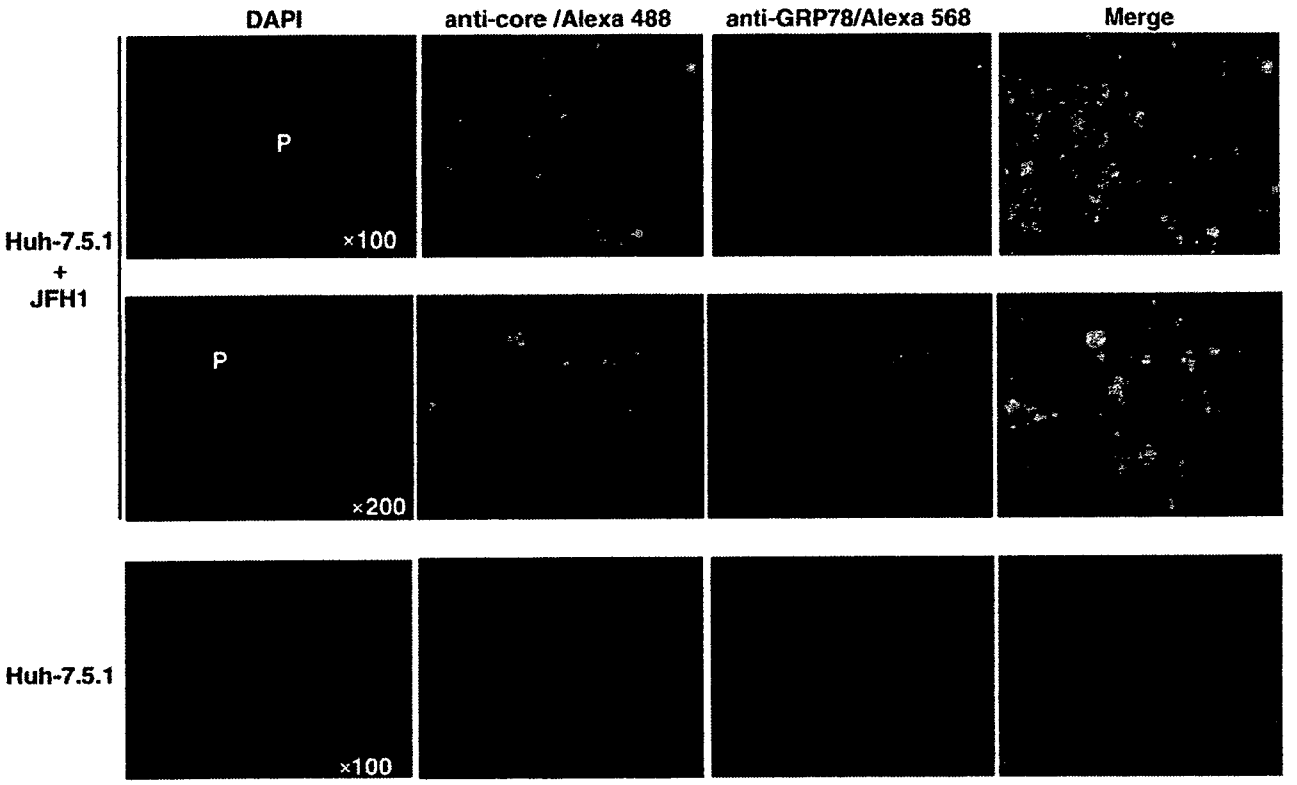

Fig. 6. Co-expression of HCV core and GRP78 in the cytopathic plaque. The HCV-JFH1 culture supernatant was transferred onto uninfected Huh-7.5.1 cells plated on 22-mm round micro cover glasses in 60-mm-diameter plates at density of 4×10^5 cells per plate. After ~5 h incubation, the supernatant was replaced with medium containing 0.8% methylcellulose. Double immunofluorescence was performed 10 days after infection using mouse anti-core antibody and goat-anti-GRP78 antibody.

Introduction of NS5B mutations in JFH1 clone showed higher replication efficiency and cytopathogenicity

We finally investigated on phenotypes of the amino acid mutations identified in the isolated cytopathic subclones. We constructed mutant clones from the wild type JFH1 plasmid, in which three amino acid mutations in NS5B region were individually introduced; T7662A, C9153T, and G9295C (see Tables 2 and 3). Transfection of the mutant HCV-RNAs showed that all mutants developed massive cell death on 10 days after transfection and that their extents of the CPE were apparently greater than the wild type JFH1 clone (Fig. 9A). The levels of core antigen in the culture medium were significantly higher in the mutant clones than in the wild type (Fig. 9B). Furthermore, the expression levels of cellular HCV core protein were significantly higher in the mutant clones than in the wild type with the order of T7662>C9153≫G9295C>JFH1 (Fig. 9C).

Discussions

Our results show that replication of HCV-JFH1 resulted in morphologic changes to the host cells, which are characterized by massive cell death (Figs. 1–3). These observations suggested that HCV infection and replication could cause CPE on the host cells. The development of the CPE involved virus protein-induced ER stress and subsequent apoptotic cell death (Figs. 4–6). The JFH1/ΔE1-E2 with deletion of the HCV envelope proteins-infected Huh-7.5.1 cells did not induce the CPE (Fig. 2A), which indicates that the key factors of plaque formation are not only viral replication but also the propagation of virus particles and re-infection. We took advantage of the HCV-induced CPE and developed a plaque assay using highly permissive Huh-7.5.1 cells. The assay revealed that the HCV-induced cytopathogenicity varied between infectious foci with cytopathic and noncytopathic infection (Fig. 3B). Interestingly, isolated JFH1 subclones from the plaques showed significantly increased infectivity and cytopathogenicity (Table 1 and Fig. 8). Viral genetic analyses showed nine amino acid substitutions; among them five were clustered in the C terminal half of the NS5B region, which might contribute to virus replication efficiency and cytopathogenicity (Table 2).

Cytopathic effects are key characteristics of the *Flaviviridae* that include Japanese encephalitis virus (JEV) (Vaughn and Hoke, 1992), West Nile Virus (Borisevich et al., 2006), yellow fever virus (Quaresma et al., 2006), dengue virus (DEN) (Despres et al., 1993), and bovine viral diarrhea virus (BVDV) (Mendez et al., 1998) and also of viruses such as adenovirus (Shinoura et al., 1999), Epstein–Barr virus (Sato et al., 1989), poliovirus (Yanagiya et al., 2005), and influenza virus (Hinshaw et al., 1994). The *Flaviviridae* utilizes the ER as the primary site for genomic replication and protein synthesis (Jordan et al., 2002; Su et al., 2002; Tardif et al., 2004). It has been reported that apoptotic cell death mediated by virus-induced ER stress contributes to the cytotoxicity of JEV, BVDV, and DEN-2

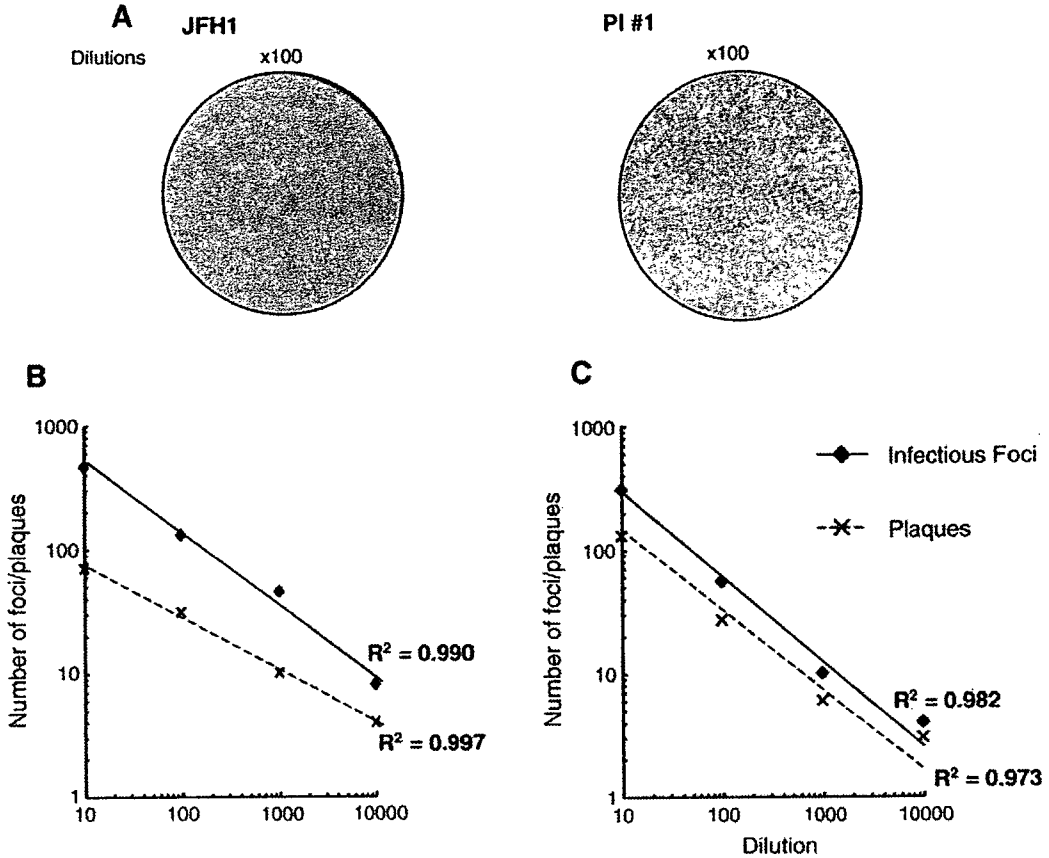

Fig. 7. Correlation of infectious foci or plaques with dilution of an inoculum. (A) Plaque assay. Huh-7.5.1 cells were seeded in collagen-coated 60-mm-diameter plates at density of 4×10^5 cells per plates and were incubated at 37 °C under 5.0% CO_2. After overnight incubation, HCV-JFH1 (left panel) or plaque-purified clone (PI #1) (right panel) infected culture supernatants were serially diluted in a final volume of 2 ml per plates and transferred onto the cell monolayers. After ~5 h of incubation, the inocula were removed, and the cell monolayers were overlaid with 8 ml of culture medium containing 0.8% methylcellulose. After 7 days of culture under normal conditions, formation of cytopathic plaque was visualized by staining with 0.08% crystal violet. (B and C) The PFU-adjusted culture supernatant of parental HCV-JFH1 (B) or plaque-purified clone (PI #1) (C) was transferred at various dilutions onto uninfected Huh-7.5.1 cells, and the plaque assay and immunocytochemistry were performed (described above). The infectivity and cytotoxicity were quantified by counting HCV-positive foci and cytopathic plaque respectively. The horizontal axis showed dilutions of the viral supernatant and the vertical axis showed the number of infectious foci or plaques.

(Jordan et al., 2002; Su et al., 2002; Yu et al., 2006). In DEN-2-infected cells, the NS2B-3 protein causes XBP1 splicing and induces ER stress (Yu et al., 2006). These findings are consistent with our results for HCV in that the JFH1 infection induced ER stress and unfolded protein responses and led to apoptotic cell death and formation of plaques.

The ER is closely associated with viral replication and assembly. Most of the HCV structural and nonstructural proteins accumulate in the ER membrane and form a membranous web that is characterized by a convoluted ER structure (Gosert et al., 2003). Moreover, the folding and assembly of HCV proteins require interaction with ER chaperone proteins such as calreticulin, BiP/GRP78, and heat shock protein-90 (HSP90) (Choukhi et al., 1998; Waxman et al., 2001). The ER stress, which is induced by virus replication, involves three different mechanisms (Tardif et al., 2002): transcriptional induction, translational attenuation, and protein degradation. In our study, both GRP78 and phosphorylated eIF2-alpha proteins were induced as viral proteins increased in concentration in HCV-JFH1 infected cells, and the GRP78 or annexin V and HCV core proteins co-localize in cytopathic plaques, showing that HCV infection and replication induce UPR and that ER stress-mediated apoptosis causes the viral cytopathic effects on host cells.

Several HCV structural and nonstructural proteins are involved in the ER stress. The structural glycoproteins, E1 and E2, interact with ER chaperones (Choukhi et al., 1998; Liberman et al., 1999), HCV NS4B induces UPR through ATF6 or the IRE1-XBP1 pathway (Zheng et al., 2005), and HCV core triggers apoptosis by inducing ER stress and ER calcium depletion both *in vitro* and *in vivo* (Benali-Furet et al., 2005).

Table 1
Cytopathogenicity and infectivity of JFH1 clones

	PFU/ml[a]	FFU/ml[b]	PFU/FFU
JFH1	$9.7\pm3.8\times10^2$[c]	$5.6\pm0.9\times10^3$	0.17±0.05
PI #1	$3.0\pm1.9\times10^3$	$4.9\pm1.6\times10^3$	0.58±0.21

[a] PFU, plaque-forming unit.
[b] FFU, focus-forming unit.
[c] Values are displayed as mean±S.D.

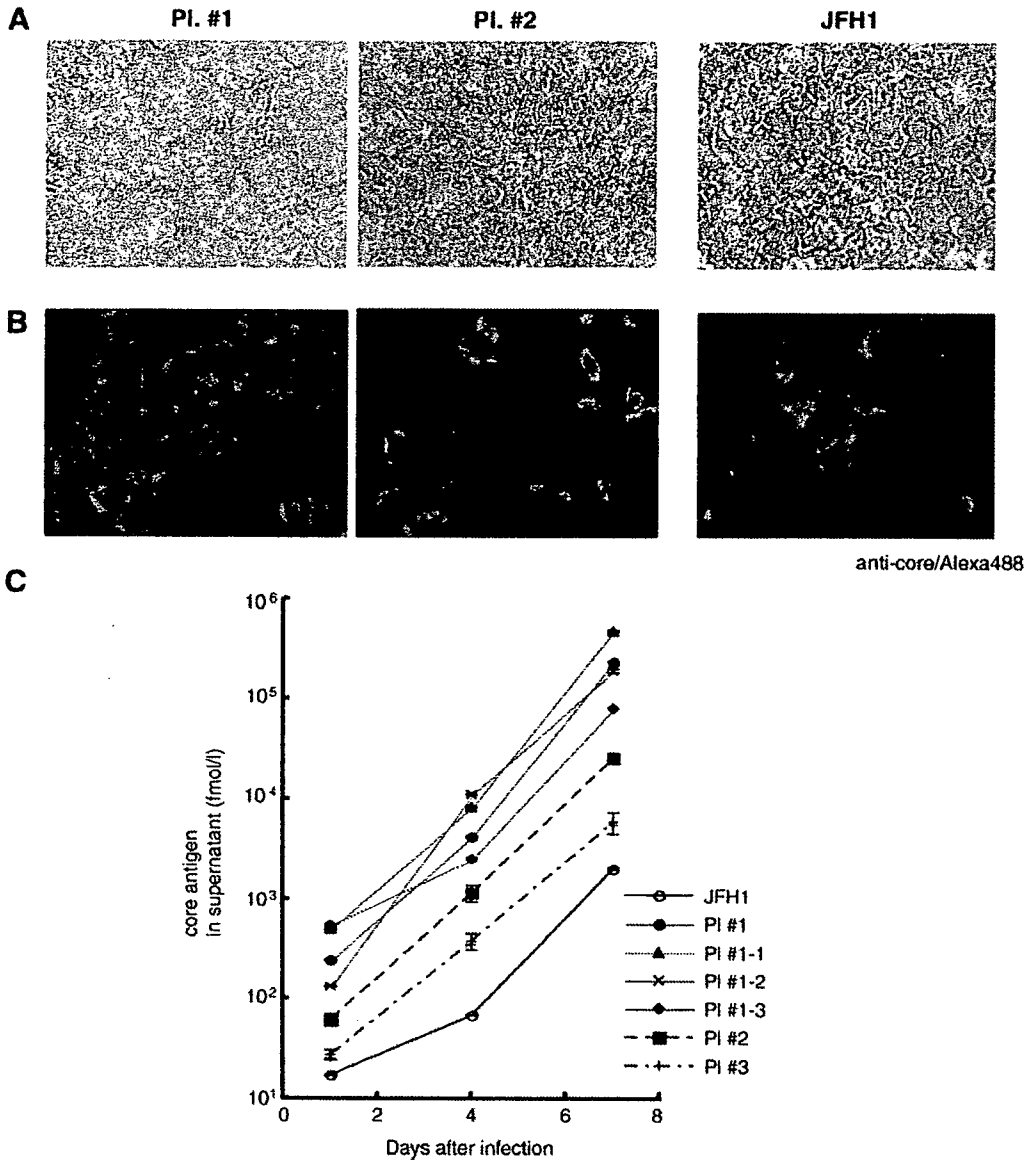

Fig. 8. The isolation of cytopathic plaques. The HCV-JFH1 culture supernatant was transferred at various dilutions onto uninfected Huh-7.5.1 cells. After ~ 5 h incubation, the supernatant was removed then infected cells were cultured in 0.8% methylcellulose-containing medium in 60-mm-diameter plates. Cytopathic plaques were detectable at 8 days after infection. Cells from each plaque were isolated using a cloning cylinder, subcultured, and transferred onto uninfected Huh-7.5.1 cells. (A) Observation by phase-contrast microscopy at 10 days of culture. (B) After 15 days of culture, the supernatant was transferred onto uninfected Huh-7.5.1 cells and an immunofluorescence assay was performed 5 days after infection using anti-core antibody. (C) Supernatants from parental JFH1, plaque-derived viruses (Pl #1, #2, and #3) and the second round isolation of plaques from the Pl #1 subclones (Pl #1-1, #1-2, and #1-3) were inoculated onto Huh-7.5.1 cells with PFU-adjusted doses, respectively. HCV core antigen levels in culture medium were measured on the days indicated. Inoculation and the assays were done in triplicate. The S.D.s were within 4% in each plot.

HCV E2 induces ER stress at lower levels but binds to PERK and inhibits phosphorylation of eIF2-alpha at high levels of expression (Pavio et al., 2003). These reports have shown that HCV may induce ER stress and regulate subsequent intracellular responses to promote its survival in hepatocytes. Consistently with these reports, our findings that HCV-JFH1 induces the expression of an ER chaperon protein and phosphorylation of eIF2-alpha indicates that robust replication of HCV-JFH1 produces unfolded proteins in the ER, leading to activation of ATF6 and stimulation of the transcription of ER chaperon proteins to promote protein folding. HCV-JFH1-induced unfolded proteins also activate PERK, which phosphorylates eIF2-alpha to inhibit the protein translation. Furthermore, the severe ER stress finally activates apoptosis signaling pathways at the early stage of viral infection. Although which HCV-JFH1 gene product is involved in ER stress-mediated apoptosis is not identified in our study, such proteins may contribute to the regulation of ER stress signaling in the host cell that leads to viral survival or cell death.

The plaque assay is often used to quantify virus infectious titers by visualizing the viral-induced CPE. However, due to the noncytopathic nature of HCV and the lack of highly permissive

Table 2
Nucleotide changes and amino acid substitutions in the cytopathic JFH1 subclone

Nucleotide[a]	Amino acid[a]
A1353G	M334V
C2842A	T843K
G3402A	G1017S
A5819G	Synonymous
T7662A	C2438S
C9153T	P2934S
G9232A	G2960D
G9293C	Synonymous
G9295C	R2985P
C9353A	H3000Q
G9355A	S3001N

[a] Nucleotide and amino acid numbers were derived from pJFH1full (Wakita et al., 2005).

host cell lines, detection of HCV-infected cells commonly relied on visualization of the infected focus by immunostaining HCV proteins (Zhong et al., 2005). Disadvantages include the costs of the antibodies and substrate, additional steps for assay and detection, and microscopic examination to count the foci. By using a highly permissive host cell line and optimizing several conditions, we have developed a plaque assay for HCV. Because the HCV-JFH1 strain is not absolutely cytopathic and does not kill all infected cells, the calculated plaque-forming units do not directly reflect HCV infectious titer but rather reflect cytopathogenicity or the percentage of cytopathic clones in the total infectious foci.

The HCV plaque assay revealed that JFH1 infection and replication developed cytopathic and noncytopathic infectious cell foci (Fig. 3B). One would suspect that the different outcomes of HCV replication might be attributable to the clonal heterogeneity of the host cells. However, there are several pieces of evidence that the Huh-7.5.1 cell line, which we used as host, might be a homogenous cell line. Huh-7.5.1 is derived from parental Huh7 cells through two rounds of clonal selection for neomycin resistance that were dependent on permissiveness for the HCV subgenomic replicon (Blight et al., 2002; Zhong et al., 2005). Sumpter et al. have reported that the HCV-permissive feature is due to mutational inactivation of RIG-I, a cytoplasmic double-stranded RNA sensor that induces type-I IFN production (Sumpter et al., 2005). This evidence suggests that the cytopathic HCV replication is attributable to virus factors, in particular, virus genomic alteration and not by clonal variation or evolution of the host cells.

Indeed, the isolation of the plaque-forming HCV subclones and inoculation onto naive cells showed significantly higher replication yields (Fig. 8) and more frequent development of cytopathic plaques (Table 1). These findings indicate that HCV-JFH1 has evolved into cytopathic and noncytopathic subclones. Our results are similar to BVDV infection. BVDV is divided into two biotypes, cytopathic (*cp*) and noncytopathic (*ncp*) strains. Most *cp* strains, which induce strong apoptotic cell death upon infection, develop from the *ncp* strains by RNA recombination such as insertion of cellular sequences, duplications and rearrangements, and deletions and lead to expression of the NS3 protein (Meyers and Thiel, 1996). Kummerer et al. have reported that other *cp* strain had point mutations in NS2 that enhanced cleavage of NS2/3 junction and NS3 production (Kummerer and Meyers, 2000). As for HCV, considering a rapid HCV replication cycle and the poor fidelity of the viral NS5B RNA-dependent RNA polymerase (RdRp) (Bartenschlager and Lohmann, 2000; Kato et al., 2005), evolution of sequence variants may well develop even after a transfection of cloned HCV-RNA. Very recently, *in vitro* permissive subclones of HCV genotype 1a, H77S stain, have been reported, which have five cell culture-adaptive mutations in the NS3, 4A, and 5A regions (Yi et al., 2007). In these clones, introduction of amino acid substitutions in the p7 and NS2 region enhanced production of the virion particles.

Interestingly, sequence analyses of a cytopathic HCV-JFH1 subclone (Pl #1) identified six amino acid substitutions in the NS5B RdRp (Table 2). Three of the six mutations were redundantly appeared in other clones that were independently isolated from the plaques (Table 3). These findings make us speculate that these amino acid substitutions may affect the enzymatic activity of RdRp by altering tertiary structure of the

Table 3
Nucleotide changes and amino acid substitutions in the NS5B regions of the cytopathic JFH1 subclones

Pl #1	#1-1	#1-2	#1-3	Pl #2	Pl #3	Pl #4
						T7623A (S2428T)
T7662A (C2438S)	T7662A (C2438S)	T7662A (C2438S)	T7662A (C2438S)	T7662A (C2438S)	T7662A (C2438S)	
					A7550C	
					C7551A (N2470T)	
						G8259C
						C8260G (A2640R)
C9153T (P2934S)	C9153T (P2934S)	C9153T (P2934S)	C9153T (P2934S)		C9153T (P2934S)	
				G9162T (V2941L)		
					A9201T (I2954F)	
G9232A (G2960D)						
				G9235A (R2965Q)		
G9295C (R2985P)	G9295C (R2985P)		G9295C (R2985P)			
C9353A (H3000Q)	C9353A (H3000Q)					
G9355A (S3001N)	G9355A (S3001N)		G9355A (S3001N)			G9355A (S3001N)

Nucleotide and amino acid numbers were derived from pJFH1full (Wakita et al., 2005).

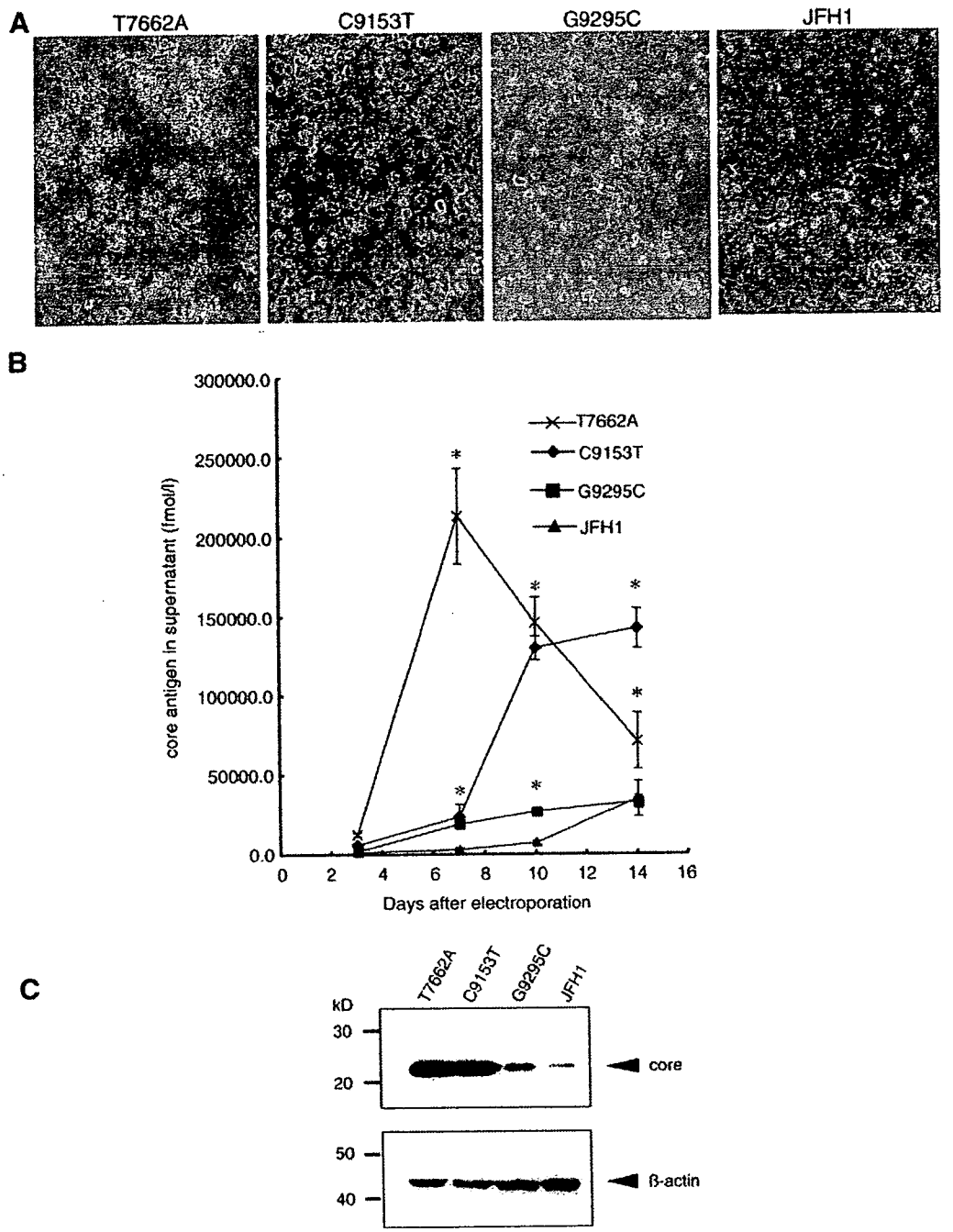

Fig. 9. Introduction of various mutations into the NS5B region of JFH1. The mutations identified in the cytopathic plaque Pl #1; T7662A, C9153T, and G9295C were introduced individually into the parental JFH1. Each JFH1 mutant, T7662A, C9153T, and G9295C, RNA was transfected into Huh-7.5.1 cells by electroporation. The transfected cells were split every 3 to 5 days (see Materials and methods). (A) JFH1 mutants transfected Huh-7.5.1 cells were observed by phase-contrast microscopy at day 7 after transfection. (B) Levels of core antigen in the culture supernatants. The culture supernatants of transfected cells were collected on the days indicated, and the levels of core antigen were measured. Asterisks indicate p-values of less than 0.05. (C) The supernatants of JFH1 mutants transfected Huh-7.5.1 cells were transferred onto uninfected Huh-7.5.1 cells. The cells were harvested at 7 days after infection. Western blotting was performed using anti-core and anti-beta-actin.

thumb domain or affect the quaternary structure of the whole HCV replicase complex by altering surface affinity to other nonstructural proteins. Mapping of the amino acid substitutions in the RdRp tertiary structure has shown that the amino acid 2438 was located on the finger domain, and three amino acids, 2934, 2960, and 2985, were located on the outer surface of the thumb domain, which corresponds to the opposite side of the nucleotide tunnel. The other substitutions, 3000 and 3001, were within the domain of the polypeptide linking the polymerase to the membrane anchor (Lesburg et al., 1999). Very

recently, Zhong et al. have reported that long-term culture of HCV-JFH1 of more than 60 days leads to the evolution of certain mutations in the viral genome (Zhong et al., 2006). They identified amino acid changes in Core, E2, NS3, and NS5A regions, and especially E2 mutation increased infectivity and density changes of viruses. In our present study, however, we could not find those mutations in the virus subclones that we have isolated in the plaque assay technique. The discrepancy might be attributable to the presence or absence of HCV-CPE-induced cell clonal alteration of the host Huh-7.5.1 that occurs concomitantly with viral genetic evolution during long-term cell culture. Further analyses may be necessary to determine the most critical regions that regulate the viral replication efficiency and cytopathogenicity.

Interestingly, the mutant virus clones, T7662A (C2438S), C9153T (P2934S), and G9295C (R2985P), showed considerably higher replication efficiency and cytopathogenicity than the wild type JFH1 clone (Fig. 9). These results strongly suggest that certain NS5B mutations in the plaque-purified strains display more replication-efficient and cytopathic phenotypes. The present data are still preliminary. Further studies may be necessary to fully characterize these mutations and their functions, which include introduction of mutations of the HCV region and of the other plaque-purified viruses and combination of the mutations, and to study their effects on virus protein functions. We are at present analyzing derivative JFH1 clones in which other amino acid mutations were introduced.

Several clinical findings have suggested that HCV is not cytopathic and that antiviral immune responses such as cytotoxic T lymphocytes play important roles in HCV pathogenesis (Cerny and Chisari, 1999). On the other hand, apoptotic cell death is the first cellular response to many hepatotoxic events and has been implicated in the pathogenesis of liver diseases, such as viral hepatitis, autoimmune diseases, alcohol-induced injury, cholestasis, hepatocellular carcinoma, and fulminant hepatic failure (Canbay et al., 2004; Ghavami et al., 2005; Patel and Gores, 1995; Rodrigues et al., 2000; Rust and Gores, 2000; Thompson, 1995). Several clinical studies have shown that fulminant hepatic failure (FHF), from which HCV-JFH1 strain was isolated, showed far more hepatocyte apoptosis, as characterized by caspase activation and Fas-FasL expression, than chronic hepatitis and normal populations (Leifeld et al., 2006; Mita et al., 2005; Ryo et al., 2000). The ER stress markers GRP78 and ATF6 are upregulated in the HCV liver tissue as the histological grade advanced. In addition, GRP78 and ATF6 are upregulated as the histological grade increased in hepatocellular carcinoma (HCC) (Shuda et al., 2003) and proteomic analysis of HCC tissue samples has shown significant upregulation of HSP70 and GRP78 (Chuma et al., 2003; Takashima et al., 2003), indicating that these proteins may play important roles in HCV-induced hepatocarcinogenesis.

In conclusion, the cytopathic mutants of HCV-JFH1 strain were isolated by using plaque assay techniques. A mechanism of the cytopathic effects involved ER stress-mediated apoptosis that was triggered by virus infection. That process of cytopathic effects might explain one aspect of HCV-induced liver injury during acute infection. Further analyses of cellular effects on HCV replication may elucidate the pathogenesis of HCV infection and may define novel host factors as targets of antiviral chemotherapeutics.

Materials and methods

Reagents

Recombinant human interferon alpha-2b was from Schering-Plough (Kenilworth, NJ). Beta-mercaptoethanol was from Wako (Osaka, Japan). Anti-CD81 antibody (JS-81) was from BD Biosciences (Franklin Lakes, NJ) (Morikawa et al., 2007).

Cells and cell culture

Huh-7.5.1 cells (Zhong et al., 2005) (kindly provided by Dr Francis V. Chisari) were maintained in Dulbecco's modified minimal essential medium (DMEM, Sigma) supplemented with 2 mmol/l L-glutamine and 10% fetal bovine serum at 37 °C under 5.0% CO_2.

In vitro RNA synthesis and transfection

A plasmid, pJFH1-full (Wakita et al., 2005), which encodes the full-length HCV-JFH1 sequence, and two control plasmids for pJFH1-full were used; pJFH1/GND that is a replication incompetent mutant with a mutation in the NS5B GDD motif and pJFH1/ΔE1-E2 in which a coding region of the HCV envelope proteins was deleted. The HCV RNA was synthesized using the RiboMax Large Scale RNA Production System (Promega, Madison, WI), with the linearized pJFH1 plasmid as template. After DNaseI (RQ-1 RNase-free DNase, Promega) treatment, the transcribed HCV-RNA was purified using ISOGEN (Nippon Gene, Tokyo, Japan). For the RNA transfection, Huh-7.5.1 cells were washed twice, and 5×10^6 cells were resuspended in Opti-MEM I (Invitrogen, Carlsbad, CA) containing 10 μg of HCV RNA, transferred into a 4-mm electroporation cuvette, and subjected to an electric pulse (1050 μF and 270 V) using the Easy Ject system (EquiBio, Mieddlesex, UK). After electroporation, the cell suspension was left for 5 min at room temperature and then incubated under normal culture conditions in a 10-cm diameter cell culture dish. The transfected cells were split every 3 to 5 days. The culture supernatants were subsequently transferred onto uninfected Huh-7.5.1 cells. The levels of HCV replication and viral protein expression were detected by real-time PCR, western blotting, and immunocytochemistry.

HCV subgenomic replicon constructs

HCV subgenomic replicon plasmid pRep-Feo was derived from the HCV-N strain pHCV1bneo-delS (Tanabe et al., 2004) and pSGR-JFH1 was from the HCV-JFH1 strain (Kato et al., 2003). The replicon RNA was synthesized from pRep-Feo or pSGR-JFH1 and transfected into Huh-7.5.1 cells. After culture in the presence of G418 (Wako), cell lines stably expressing the replicon were established.

Real-time RT-PCR analysis

Total cellular RNA was isolated using ISOGEN (Nippon Gene). Two micrograms of total cellular RNA was used to generate cDNA from each sample using SuperScript II (Invitrogen) reverse transcriptase. Expression of mRNA was quantified using Quanti Tect SYBR Green PCR Master Mix (QIAGEN, Valencia, CA) and the ABI 7500 Real-Time PCR System (Applied Biosystems, Foster City, CA). The primers used were as follows: HCV-JFH1 sense (positions 7090 to 7109; 5′-TCA GAC AGA GCC TGA GTC CA-3′), HCV-JFH1 antisense (positions 7404 to 7423; 5′-AGT TGC TGG AGG GCT TCT GA-3′), beta-actin sense (5′-ACA ATG AAG ATC AAG ATC ATT GCT CCT CCT-3′), and beta-actin antisense (5′-TTT GCG GTG GAC GAT GGA GGG GCC GGA CTC-3′).

Quantification of HCV core antigen in the culture supernatant

The culture supernatants of JFH1-RNA transfected Huh-7.5.1 cells were collected on the days indicated, passed through a 0.45 μm filter (MILLEX-HA, Millipore, Bedford, MA), and stored at −80 °C. The levels of core antigen in the culture supernatants were measured using a chemiluminescence enzyme immunoassay (CLEIA) according to the manufacturer's protocol (Lumipulse Ortho HCV Antigen, Ortho-Clinical Diagnostics, Tokyo, Japan).

Western blotting

Western blotting was carried out as described previously (Tanabe et al., 2004; Yokota et al., 2003). Briefly, 10 μg of total cell lysate was separated by SDS–PAGE and blotted onto a polyvinylidene fluoride (PVDF) western blotting membrane. The membrane was incubated with the primary antibodies followed by a peroxidase-labeled anti-IgG antibody and visualized by chemiluminescence using the ECL western blotting Analysis System (Amersham Biosciences, Buckinghamshire, UK). The antibodies used were anti-core mouse monoclonal antibody 2H9 (provided by Dr. Wakita), anti-GRP78 goat monoclonal antibody, anti-GADD153/CHOP rabbit polyclonal antibody (Santa Cruz Biotechnology, Santa Cruz, CA), anti-eIF2-alpha, anti-phospho-eIF2-alpha rabbit polyclonal antibody (Cell Signaling, Danvers, CA), and anti-beta-actin antibody (Sigma).

Immunocytochemistry

HCV-JFH1-transfected or infected Huh-7.5.1 cells were cultured in Lab-Tek® Chamber Slide™ (Nalge Nunc International, Rochester, NY) or on 22-mm-round micro cover glasses (Matsunami, Tokyo, Japan). For detection of HCV-core and GRP78, cells were fixed with cold acetone for 15 min. The cells were incubated with the primary antibodies for 1 h at 37 °C and with Alexa Fluor 488 goat anti-mouse IgG antibody or Alexa Fluor 568 donkey anti-goat IgG antibody (Molecular Probes, Eugene, OR) for 1 h at room temperature. To analyze apoptosis of HCV-JFH1 infected cells, double staining for annexin V-FITC binding and for cellular DNA using propidium iodide (PI) was performed using an annexin V-Fluorescein Staining Kit (Wako, Osaka, Japan). Cells were visualized by a fluorescence microscopy (BZ-8000, KEYENCE, Osaka, Japan).

Plaque assay

Huh-7.5.1 cells were seeded in collagen-coated 60-mm-diameter plates at a density of $2–4 \times 10^5$ cells per plates and were incubated at 37 °C under 5.0% CO_2 (as described above). After overnight incubation, HCV-infected culture supernatants were serially diluted in a final volume of 2 ml per plates and transferred onto the cell monolayers. After ~5 h of incubation, the inocula were removed, and the cell monolayers were overlaid with 8 ml of culture medium (DMEM, 2 mmol/l L-glutamine and 10% fetal bovine serum) that contained 0.8% methylcellulose. After 7 to 12 days of incubation under normal culture conditions, formation of cytopathic plaque was visualized by staining the cell monolayers with 0.08% crystal violet solution (Sigma). The levels of cytotoxicity were evaluated by counting the plaques and calculating the titer (PFU/ml). Similarly, the titers of infectivity were evaluated by performing immunocytochemistry to detect foci of HCV-core-positive cells and calculating the infectious focus-forming units (FFU/ml).

Sequence analyses

The cDNA from the isolated JFH1 plaque was amplified from cytopathic virus-infected Huh-7.5.1 cells by RT-PCR and subjected to direct sequence determination. Nucleotide sequences were read from both strands using Big Dye Terminator Cycle Sequencing Ready Reaction kits (Applied Biosystems) and an automated DNA sequencer (ABI PRISM® 310 Genetic Analyzer; Applied Biosystems).

Establishment of mutant JFH1 clones

In order to introduce various mutations into the NS5B region of JFH1, plasmid pJFH1 was digested with *Hin*dIII and the DNA fragment encompassing nt. 8231 to 9731 was subcloned into the pBluescriptII SK+ phagemid vector (Stratagene, La Jolla, CA). The following mutations were introduced into the DNA fragment in the subcloning vector by site-directed mutagenesis (Quick-ChangeII Site-Directed Mutagenesis Kit; Stratagene): C9153T and G9295C, respectively. Finally, these *Hin*dIII–*Hin*dIII fragments were subcloned back into the parental plasmid pJFH1. The mutation T7662A-introduced PCR fragment (nt. 7421–7839) was subcloned into the T-Vector (pGEM-T Easy Vector Systems; Promega) and digested with *Rsr*II and *Bsr*GI. Finally, these *Rsr*II–*Bsr*GI fragments were subcloned back into the parental plasmid.

Statistical analyses

Statistical analyses were performed using the Student's *t*-test, and *p*-values of less than 0.05 were considered as statistically significant.

Acknowledgments

We are indebted to Dr. Francis V. Chisari for providing the Huh-7.5.1 cell line. This study was supported by grants from the Japan Society for the Promotion of Science, Miyakawa Memorial Research Foundation, and Viral Hepatitis Research Foundation of Japan.

References

Bartenschlager, R., Lohmann, V., 2000. Replication of hepatitis C virus. J. Gen. Virol. 81 (Pt 7), 1631–1648.

Benali-Furet, N.L., Chami, M., Houel, L., De Giorgi, F., Vernejoul, F., Lagorce, D., Buscail, L., Bartenschlager, R., Ichas, F., Rizzuto, R., Paterlini-Brechot, P., 2005. Hepatitis C virus core triggers apoptosis in liver cells by inducing ER stress and ER calcium depletion. Oncogene 24 (31), 4921–4933.

Blight, K.J., Kolykhalov, A.A., Rice, C.M., 2000. Efficient initiation of HCV RNA replication in cell culture. Science 290 (5498), 1972–1974.

Blight, K.J., McKeating, J.A., Rice, C.M., 2002. Highly permissive cell lines for subgenomic and genomic hepatitis C virus RNA replication. J. Virol. 76 (24), 13001–13014.

Borisevich, V., Seregin, A., Nistler, R., Mutabazi, D., Yamshchikov, V., 2006. Biological properties of chimeric West Nile viruses. Virology 349 (2), 371–381.

Canbay, A., Friedman, S., Gores, G.J., 2004. Apoptosis: the nexus of liver injury and fibrosis. Hepatology 39 (2), 273–278.

Cerny, A., Chisari, F.V., 1999. Pathogenesis of chronic hepatitis C: immunological features of hepatic injury and viral persistence. Hepatology 30 (3), 595–601.

Choukhi, A., Ung, S., Wychowski, C., Dubuisson, J., 1998. Involvement of endoplasmic reticulum chaperones in the folding of hepatitis C virus glycoproteins. J. Virol. 72 (5), 3851–3858.

Chuma, M., Sakamoto, M., Yamazaki, K., Ohta, T., Ohki, M., Asaka, M., Hirohashi, S., 2003. Expression profiling in multistage hepatocarcinogenesis: identification of HSP70 as a molecular marker of early hepatocellular carcinoma. Hepatology 37 (1), 198–207.

Despres, P., Frenkiel, M.P., Deubel, V., 1993. Differences between cell membrane fusion activities of two dengue type-1 isolates reflect modifications of viral structure. Virology 196 (1), 209–219.

Despres, P., Flamand, M., Ceccaldi, P.E., Deubel, V., 1996. Human isolates of dengue type 1 virus induce apoptosis in mouse neuroblastoma cells. J. Virol. 70 (6), 4090–4096.

Ferri, K.F., Kroemer, G., 2001. Organelle-specific initiation of cell death pathways. Nat. Cell Biol. 3 (11), E255–E263.

Ghavami, S., Hashemi, M., Kadkhoda, K., Alavian, S.M., Bay, G.H., Los, M., 2005. Apoptosis in liver diseases—detection and therapeutic applications. Med. Sci. Monit. 11 (11), RA337–RA345.

Gosert, R., Egger, D., Lohmann, V., Bartenschlager, R., Blum, H.E., Bienz, K., Moradpour, D., 2003. Identification of the hepatitis C virus RNA replication complex in Huh-7 cells harboring subgenomic replicons. J. Virol. 77 (9), 5487–5492.

Harding, H.P., Zhang, Y., Ron, D., 1999. Protein translation and folding are coupled by an endoplasmic-reticulum-resident kinase. Nature 397 (6716), 271–274.

He, B., 2006. Viruses, endoplasmic reticulum stress, and interferon responses. Cell Death Differ. 13 (3), 393–403.

Hinshaw, V.S., Olsen, C.W., Dybdahl-Sissoko, N., Evans, D., 1994. Apoptosis: a mechanism of cell killing by influenza A and B viruses. J. Virol. 68 (6), 3667–3673.

Jordan, R., Wang, L., Graczyk, T.M., Block, T.M., Romano, P.R., 2002. Replication of a cytopathic strain of bovine viral diarrhea virus activates PERK and induces endoplasmic reticulum stress-mediated apoptosis of MDBK cells. J. Virol. 76 (19), 9588–9599.

Kato, T., Furusaka, A., Miyamoto, M., Date, T., Yasui, K., Hiramoto, J., Nagayama, K., Tanaka, T., Wakita, T., 2001. Sequence analysis of hepatitis C virus isolated from a fulminant hepatitis patient. J. Med. Virol. 64 (3), 334–339.

Kato, T., Date, T., Miyamoto, M., Furusaka, A., Tokushige, K., Mizokami, M., Wakita, T., 2003. Efficient replication of the genotype 2a hepatitis C virus subgenomic replicon. Gastroenterology 125 (6), 1808–1817.

Kato, N., Nakamura, T., Dansako, H., Namba, K., Abe, K., Nozaki, A., Naka, K., Ikeda, M., Shimotohno, K., 2005. Genetic variation and dynamics of hepatitis C virus replicons in long-term cell culture. J. Gen. Virol. 86 (Pt 3), 645–656.

Kaufman, R.J., 1999. Stress signaling from the lumen of the endoplasmic reticulum: coordination of gene transcriptional and translational controls. Genes Dev. 13 (10), 1211–1233.

Koutsoudakis, G., Herrmann, E., Kallis, S., Bartenschlager, R., Pietschmann, T., 2007. The level of CD81 cell surface expression is a key determinant for productive entry of hepatitis C virus into host cells. J. Virol. 81 (2), 588–598.

Kummerer, B.M., Meyers, G., 2000. Correlation between point mutations in NS2 and the viability and cytopathogenicity of Bovine viral diarrhea virus strain Oregon analyzed with an infectious cDNA clone. J. Virol. 74 (1), 390–400.

Leifeld, L., Nattermann, J., Fielenbach, M., Schmitz, V., Sauerbruch, T., Spengler, U., 2006. Intrahepatic activation of caspases in human fulminant hepatic failure. Liver Int. 26 (7), 872–879.

Lesburg, C.A., Cable, M.B., Ferrari, E., Hong, Z., Mannarino, A.F., Weber, P.C., 1999. Crystal structure of the RNA-dependent RNA polymerase from hepatitis C virus reveals a fully encircled active site. Nat. Struct. Biol. 6 (10), 937–943.

Liberman, E., Fong, Y.L., Selby, M.J., Choo, Q.L., Cousens, L., Houghton, M., Yen, T.S., 1999. Activation of the grp78 and grp94 promoters by hepatitis C virus E2 envelope protein. J. Virol. 73 (5), 3718–3722.

Lindenbach, B.D., Evans, M.J., Syder, A.J., Wolk, B., Tellinghuisen, T.L., Liu, C.C., Maruyama, T., Hynes, R.O., Burton, D.R., McKeating, J.A., Rice, C.M., 2005. Complete replication of hepatitis C virus in cell culture. Science 309 (5734), 623–626.

Lohmann, V., Korner, F., Koch, J., Herian, U., Theilmann, L., Bartenschlager, R., 1999. Replication of subgenomic hepatitis C virus RNAs in a hepatoma cell line. Science 285 (5424), 110–113.

Maekawa, S., Enomoto, N., Sakamoto, N., Kurosaki, M., Ueda, E., Kohashi, T., Watanabe, H., Chen, C.H., Yamashiro, T., Tanabe, Y., Kanazawa, N., Nakagawa, M., Sato, C., Watanabe, M., 2004. Introduction of NS5A mutations enables subgenomic HCV replicon derived from chimpanzee-infectious HC-J4 isolate to replicate efficiently in Huh-7 cells. J. Viral Hepatitis 11 (5), 394–403.

Mendez, E., Ruggli, N., Collett, M.S., Rice, C.M., 1998. Infectious bovine viral diarrhea virus (strain NADL) RNA from stable cDNA clones: a cellular insert determines NS3 production and viral cytopathogenicity. J. Virol. 72 (6), 4737–4745.

Meyers, G., Thiel, H.J., 1996. Molecular characterization of pestiviruses. Adv. Virus Res. 47, 53–118.

Mita, A., Hashikura, Y., Tagawa, Y., Nakayama, J., Kawakubo, M., Miyagawa, S., 2005. Expression of Fas ligand by hepatic macrophages in patients with fulminant hepatic failure. Am. J. Gastroenterol. 100 (11), 2551–2559.

Mori, K., 2000. Tripartite management of unfolded proteins in the endoplasmic reticulum. Cell 101 (5), 451–454.

Morikawa, K., Zhao, Z., Date, T., Miyamoto, M., Murayama, A., Akazawa, D., Tanabe, J., Sone, S., Wakita, T., 2007. The roles of CD81 and glycosaminoglycans in the adsorption and uptake of infectious HCV particles. J. Med. Virol. 79 (6), 714–723.

Mottola, G., Cardinali, G., Ceccacci, A., Trozzi, C., Bartholomew, L., Torrisi, M.R., Pedrazzini, E., Bonatti, S., Migliaccio, G., 2002. Hepatitis C virus nonstructural proteins are localized in a modified endoplasmic reticulum of cells expressing viral subgenomic replicons. Virology 293 (1), 31–43.

Munro, S., Pelham, H.R., 1986. An Hsp70-like protein in the ER: identity with the 78 kD glucose-regulated protein and immunoglobulin heavy chain binding protein. Cell 46 (2), 291–300.

Nakagawa, M., Sakamoto, N., Tanabe, Y., Koyama, T., Itsui, Y., Takeda, Y., Chen, C.H., Kakinuma, S., Oooka, S., Maekawa, S., Enomoto, N., Watanabe, M., 2005. Suppression of hepatitis C virus replication by cyclosporin a is mediated by blockade of cyclophilins. Gastroenterology 129 (3), 1031–1041.

Pahl, H.L., 1999. Signal transduction from the endoplasmic reticulum to the cell nucleus. Physiol. Rev. 79 (3), 683–701.

Patel, T., Gores, G.J., 1995. Apoptosis and hepatobiliary disease. Hepatology 21 (6), 1725–1741.

Pavio, N., Romano, P.R., Graczyk, T.M., Feinstone, S.M., Taylor, D.R., 2003. Protein synthesis and endoplasmic reticulum stress can be modulated by the hepatitis C virus envelope protein E2 through the eukaryotic initiation factor 2alpha kinase PERK. J. Virol. 77 (6), 3578–3585.

Quaresma, J.A., Barros, V.L., Pagliari, C., Fernandes, E.R., Guedes, F., Takakura, C.F., Andrade Jr., H.F., Vasconcelos, P.F., Duarte, M.I., 2006. Revisiting the liver in human yellow fever: virus-induced apoptosis in hepatocytes associated with TGF-beta, TNF-alpha and NK cells activity. Virology 345 (1), 22–30.

Rodrigues, C.M., Brites, D., Serejo, F., Costa, A., Ramalho, F., De Moura, M.C., 2000. Apoptotic cell death does not parallel other indicators of liver damage in chronic hepatitis C patients. J. Viral Hepatitis 7 (3), 175–183.

Rust, C., Gores, G.J., 2000. Apoptosis and liver disease. Am. J. Med. 108 (7), 567–574.

Ryo, K., Kamogawa, Y., Ikeda, I., Yamauchi, K., Yonehara, S., Nagata, S., Hayashi, N., 2000. Significance of Fas antigen-mediated apoptosis in human fulminant hepatic failure. Am. J. Gastroenterol. 95 (8), 2047–2055.

Sato, H., Takimoto, T., Tanaka, S., Ogura, H., Shiraishi, K., Tanaka, J., 1989. Cytopathic effects induced by Epstein–Barr virus replication in epithelial nasopharyngeal carcinoma hybrid cells. J. Virol. 63 (8), 3555–3559.

Shinoura, N., Yoshida, Y., Tsunoda, R., Ohashi, M., Zhang, W., Asai, A., Kirino, T., Hamada, H., 1999. Highly augmented cytopathic effect of a fiber-mutant E1B-defective adenovirus for gene therapy of gliomas. Cancer Res. 59 (14), 3411–3416.

Shuda, M., Kondoh, N., Imazeki, N., Tanaka, K., Okada, T., Mori, K., Hada, A., Arai, M., Wakatsuki, T., Matsubara, O., Yamamoto, N., Yamamoto, M., 2003. Activation of the ATF6, XBP1 and grp78 genes in human hepatocellular carcinoma: a possible involvement of the ER stress pathway in hepatocarcinogenesis. J. Hepatol. 38 (5), 605–614.

Su, H.L., Liao, C.L., Lin, Y.L., 2002. Japanese encephalitis virus infection initiates endoplasmic reticulum stress and an unfolded protein response. J. Virol. 76 (9), 4162–4171.

Sumpter Jr., R., Loo, Y.M., Foy, E., Li, K., Yoneyama, M., Fujita, T., Lemon, S.M., Gale Jr., M., 2005. Regulating intracellular antiviral defense and permissiveness to hepatitis C virus RNA replication through a cellular RNA helicase, RIG-I. J. Virol. 79 (5), 2689–2699.

Takashima, M., Kuramitsu, Y., Yokoyama, Y., Iizuka, N., Toda, T., Sakaida, I., Okita, K., Oka, M., Nakamura, K., 2003. Proteomic profiling of heat shock protein 70 family members as biomarkers for hepatitis C virus-related hepatocellular carcinoma. Proteomics 3 (12), 2487–2493.

Tanabe, Y., Sakamoto, N., Enomoto, N., Kurosaki, M., Ueda, E., Maekawa, S., Yamashiro, T., Nakagawa, M., Chen, C.H., Kanazawa, N., Kakinuma, S., Watanabe, M., 2004. Synergistic inhibition of intracellular hepatitis C virus replication by combination of ribavirin and interferon-alpha. J. Infect. Dis. 189 (7), 1129–1139.

Tardif, K.D., Mori, K., Siddiqui, A., 2002. Hepatitis C virus subgenomic replicons induce endoplasmic reticulum stress activating an intracellular signaling pathway. J. Virol. 76 (15), 7453–7459.

Tardif, K.D., Mori, K., Kaufman, R.J., Siddiqui, A., 2004. Hepatitis C virus suppresses the IRE1-XBP1 pathway of the unfolded protein response. J. Biol. Chem. 279 (17), 17158–17164.

Thompson, C.B., 1995. Apoptosis in the pathogenesis and treatment of disease. Science 267 (5203), 1456–1462.

Vaughn, D.W., Hoke Jr., C.H., 1992. The epidemiology of Japanese encephalitis: prospects for prevention. Epidemiol. Rev. 14, 197–221.

Wakita, T., Pietschmann, T., Kato, T., Date, T., Miyamoto, M., Zhao, Z., Murthy, K., Habermann, A., Krausslich, H.G., Mizokami, M., Bartenschlager, R., Liang, T.J., 2005. Production of infectious hepatitis C virus in tissue culture from a cloned viral genome. Nat. Med. 11 (7), 791–796.

Waxman, L., Whitney, M., Pollok, B.A., Kuo, L.C., Darke, P.L., 2001. Host cell factor requirement for hepatitis C virus enzyme maturation. Proc. Natl. Acad. Sci. U. S. A. 98 (24), 13931–13935.

Yanagiya, A., Jia, Q., Ohka, S., Horie, H., Nomoto, A., 2005. Blockade of the poliovirus-induced cytopathic effect in neural cells by monoclonal antibody against poliovirus or the human poliovirus receptor. J. Virol. 79 (3), 1523–1532.

Yi, M., Ma, Y., Yates, J., Lemon, S.M., 2007. Compensatory mutations in E1, p7, NS2, and NS3 enhance yields of cell culture-infectious intergenotypic chimeric hepatitis C virus. J. Virol. 81 (2), 629–638.

Yokota, T., Sakamoto, N., Enomoto, N., Tanabe, Y., Miyagishi, M., Maekawa, S., Yi, L., Kurosaki, M., Taira, K., Watanabe, M., Mizusawa, H., 2003. Inhibition of intracellular hepatitis C virus replication by synthetic and vector-derived small interfering RNAs. EMBO Rep. 4 (6), 602–608.

Yu, C.Y., Hsu, Y.W., Liao, C.L., Lin, Y.L., 2006. Flavivirus infection activates the XBP1 pathway of the unfolded protein response to cope with endoplasmic reticulum stress. J. Virol. 80 (23), 11868–118680.

Zheng, Y., Gao, B., Ye, L., Kong, L., Jing, W., Yang, X., Wu, Z., Ye, L., 2005. Hepatitis C virus non-structural protein NS4B can modulate an unfolded protein response. J. Microbiol. 43 (6), 529–536.

Zhong, J., Gastaminza, P., Cheng, G., Kapadia, S., Kato, T., Burton, D.R., Wieland, S.F., Uprichard, S.L., Wakita, T., Chisari, F.V., 2005. Robust hepatitis C virus infection in vitro. Proc. Natl. Acad. Sci. U. S. A. 102 (26), 9294–9299.

Zhong, J., Gastaminza, P., Chung, J., Stamataki, Z., Isogawa, M., Cheng, G., McKeating, J.A., Chisari, F.V., 2006. Persistent hepatitis C virus infection in vitro: coevolution of virus and host. J. Virol. 80 (22), 11082–11093.

JOURNAL OF VIROLOGY, Dec. 2007, p. 13922–13926 Vol. 81, No. 24
0022-538X/07/$08.00+0 doi:10.1128/JVI.01517-07

DDX3 DEAD-Box RNA Helicase Is Required for Hepatitis C Virus RNA Replication▽

Yasuo Ariumi,[1] Misao Kuroki,[1] Ken-ichi Abe,[1] Hiromichi Dansako,[1] Masanori Ikeda,[1] Takaji Wakita,[2] and Nobuyuki Kato[1]*

Department of Molecular Biology, Okayama University Graduate School of Medicine, Dentistry, and Pharmaceutical Sciences, 2-5-1, Shikata-cho, Okayama 700-8558,[1] and Department of Virology II, National Institute of Infectious Diseases, Toyama 1-23-1, Shinjuku-ku, Tokyo 162-8640,[2] Japan

Received 11 July 2007/Accepted 5 September 2007

DDX3, a DEAD-box RNA helicase, binds to the hepatitis C virus (HCV) core protein. However, the role(s) of DDX3 in HCV replication is still not understood. Here we demonstrate that the accumulation of both genome-length HCV RNA (HCV-O, genotype 1b) and its replicon RNA were significantly suppressed in HuH-7-derived cells expressing short hairpin RNA targeted to DDX3 by lentivirus vector transduction. As well, RNA replication of JFH1 (genotype 2a) and release of the core into the culture supernatants were suppressed in DDX3 knockdown cells after inoculation of the cell culture-generated HCVcc. Thus, DDX3 is required for HCV RNA replication.

DEAD-box RNA helicases are involved in various RNA metabolic processes, including transcription, translation, RNA splicing, RNA transport, and RNA degradation (9, 20). DDX1 and DDX3, DEAD-box RNA helicases, have been implicated in the replication of human immunodeficiency virus type 1 (HIV-1). Both DDX1 and DDX3 interact with HIV-1 Rev and enhance Rev-dependent HIV-1 RNA nuclear export (10, 24).

On the other hand, DDX3 binds to the hepatitis C virus (HCV) core protein (17, 19, 25), and DDX3 expression is deregulated in HCV-associated hepatocellular carcinoma (HCC) (7, 8). However, the biological function of DDX3 in HCV replication is still not understood. To address this issue, we first used lentivirus vector-mediated RNA interference to stably knock down DDX3 in three HuH-7-derived cell lines: O cells, harboring a replicative genome-length HCV RNA (HCV-O, genotype 1b) (13); sO cells, harboring its subgenomic replicon of HCV RNA (14); or RSc cured cells, which cell culture-generated HCV (HCVcc) (JFH1, genotype 2a) (23) could infect and effectively replicate in (M. Ikeda et al., unpublished data). Oligonucleotides with the following sense and antisense sequences were used for the cloning of short hairpin RNA (shRNA)-encoding sequences against DDX3 in the lentivirus vector: for DDX3i#3, 5′-GATCCCCGGAGGA AATTATAACTCCCTTCAAGAGAGGGAGTTATAATTT CCTCCTTTTTGGAAA-3′ (sense) and 5′-AGCTTTTCCAA AAAGGAGGAAATTATAACTCCCTCTCTTGAAGGGA GTTATAATTTCCTCCGGG-3′ (antisense); for DDX3i#7, 5′-GATCCCCGGTCACCCTGCCAAACAAGTTCAAGAG ACTTGTTTGGCAGGGTGACCTTTTTGGAAA-3′ (sense) and 5′-AGCTTTTCCAAAAAGGTCACCCTGCCAAACAA GTCTCTTGAACTTGTTTGGCAGGGTGACCGGG-3′ (antisense). These oligonucleotides were annealed and subcloned into the BglII-HindIII site, downstream from an RNA polymerase III promoter of pSUPER (6). To construct pLV-DDX3i#3 and pLV-DDX3i#7, the BamHI-SalI fragments of the corresponding pSUPER plasmids were subcloned into the BamHI-SalI site of pRDI292 (5), an HIV-1-derived self-inactivating lentivirus vector containing a puromycin resistance marker allowing for the selection of transduced cells. The vesicular stomatitis virus G protein (VSV-G)-pseudotyped HIV-1-based vector system has been described previously (18). We used the second-generation packaging construct pCMV-ΔR8.91 (26) and the VSV-G-envelope plasmid pMDG2. The lentivirus vector particles were produced by transient transfection of 293FT cells with FuGene 6 (Roche).

Western blot analysis of the lysates demonstrated the only trace of DDX3 protein in DDX3 knockdown O cells (DDX3i#3) (Fig. 1A). In this context, the HCV core expression level was significantly decreased in the DDX3 knockdown O cells (Fig. 1A). To further confirm this finding, we examined the level of HCV RNA in these cells. We found that accumulation of genome-length HCV-O RNA was notably suppressed in DDX3 knockdown O cells (Fig. 1B). Furthermore, the efficiency of colony formation in DDX3 knockdown Oc cells (created by eliminating genome-length HCV RNA from O cells by interferon treatment) transfected with the genome-length HCV-O RNA with an adapted mutation at amino acid (aa) position 1609 in the NS3 helicase region (K1609E) (13) was also notably reduced compared with that in control cells (Fig. 1C). In contrast, highly efficient knockdown of an unrelated host factor, poly(ADP-ribose) polymerase 1 (PARP-1) (4), had no observable effects on HCV RNA replication, the efficiency of colony formation, or the core expression level (data not shown), suggesting that our finding was not due to a nonspecific event. Interestingly, accumulation of the subgenomic replicon RNA (HCV-sO) was also suppressed in DDX3 knockdown sO cells (Fig. 1D). Moreover, we examined the potential role of DDX3 in an HCV infection and produc-

* Corresponding author. Mailing address: Department of Molecular Biology, Okayama University Graduate School of Medicine, Dentistry, and Pharmaceutical Sciences, 2-5-1, Shikata-cho, Okayama 700-8558, Japan. Phone: 81 86 235 7386. Fax: 81 86 235 7392. E-mail: nkato@md.okayama-u.ac.jp.

▽ Published ahead of print on 12 September 2007.

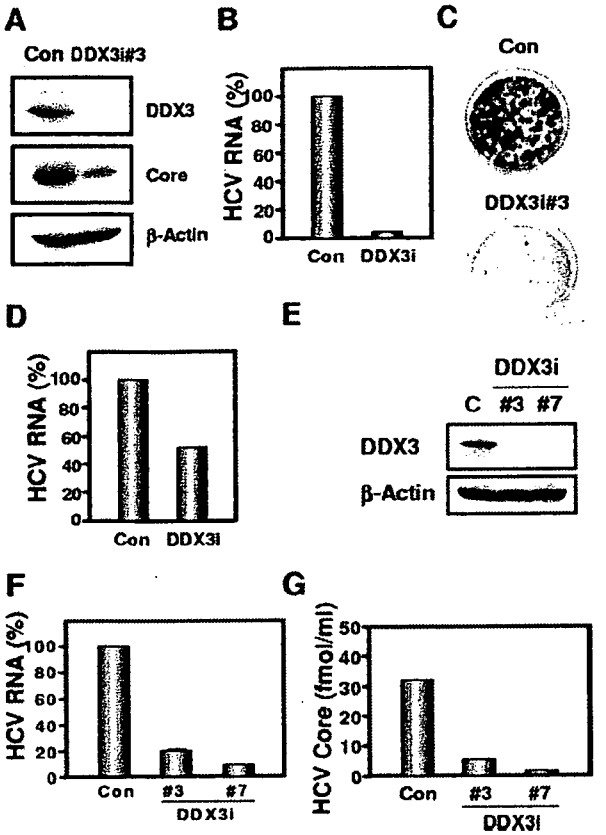

FIG. 1. Requirement of DDX3 for HCV replication. (A to D) Effect of DDX3 knockdown on HCV RNA replication. (A) Inhibition of DDX3 expression by shRNA-producing lentivirus vector. The results of Western blot analysis of cellular lysates with anti-DDX3 (ProSci), anti-HCV core (CP-9; Institute of Immunology), or an anti-β-actin antibody (Sigma) in O cells expressing shRNA against DDX3 (DDX3i#3) as well as in O cells transduced with a control lentivirus vector (Con) are shown. (B) The level of genome-length HCV RNA was monitored by real-time LightCycler PCR (Roche). Experiments were done in duplicate, and bars represent the mean percentages of HCV RNA. (C) Efficiency of colony formation in DDX3 knockdown cells. In vitro-transcribed ON/C-5B K1609E RNA (2 μg) was transfected into the DDX3 knockdown Oc cells (DDX3i#3) or the Oc cells transduced with a control lentivirus vector (Con). G418-resistant colonies were stained with Coomassie brilliant blue at 3 weeks after electroporation of RNA. Experiments were done in duplicate, and representative results are shown. (D) The level of subgenomic replicon RNA was monitored by real-time LightCycler PCR. Experiments were done in duplicate, and bars represent the mean percentages of HCV RNA. (E to G) Effect of DDX3 knockdown on HCV infection. (E) Inhibition of DDX3 expression by shRNA-producing lentivirus vector. The results of Western blot analysis of cellular lysates with anti-DDX3 or an anti-β-actin antibody for RSc cells expressing the shRNA DDX3i#3 or DDX3i#7 and for RSc cells transduced with a control lentivirus vector (Con) are shown. (F) The level of genome-length HCV (JFH1) RNA was monitored by real-time LightCycler PCR after inoculation of the cell culture-generated HCVcc. Results from three independent experiments are shown. (G) The levels of the HCV core in the culture supernatants were determined by an enzyme-linked immunosorbent assay (Mitsubishi Kagaku Bio-Clinical Laboratories). Experiments were done in duplicate, and bars represent the mean HCV core protein levels.

tion system (23). We found 80 to 90% reductions in the accumulation of JFH1 RNA and 82 to 94% reductions in the release of the core into the culture supernatants in DDX3 knockdown HuH-7-derived RSc cured cells at 4 days after inoculation of HCVcc (Fig. 1E to G). Thus, DDX3 seems to be required for HCV RNA replication.

Previously, DDX3 was identified as an HCV core-interacting protein by yeast two-hybrid screening. This interaction required the N-terminal domain of the core (aa 1 to 59) and the C-terminal domain of DDX3 (aa 553 to 622) (17, 19, 25). To determine whether the core can interact with DDX3 regardless of the HCV genotype, we used the HCV-O core (genotype 1b) and the JFH1 core (genotype 2a) (Table 1). We first examined their subcellular localization by confocal laser scanning microscopy as previously described (3). Consistent with previous reports (17, 19, 25), both the HCV-O core and JFH1 core mostly colocalized with DDX3 in the perinuclear region (Fig. 2A). Then we immunoprecipitated lysates from 293FT cells in which hemagglutinin (HA)-tagged DDX3 and HCV-O core, JFH1 core, or their 40-aa N-truncated mutants were overexpressed with an anti-HA antibody. Cells were lysed in a buffer containing 50 mM Tris-HCl (pH 8.0), 150 mM NaCl, 4 mM EDTA, 0.5% NP-40, 10 mM NaF, 0.1 mM Na_3VO_4, 1 mM dithiothreitol, and 1 mM phenylmethylsulfonyl fluoride. Lysates were precleared with 30 μl of protein G-Sepharose (GE Healthcare Bio-Sciences). Precleared supernatants were incubated with 1 μg of anti-HA antibody (3F10; Roche) at 4°C for 1 h. Following absorption of the precipitates

TABLE 1. Primers used for construction of the HCV core-expressing plasmids[a]

Plasmid name	Direction	Primer sequence
pCXbsr/core(HCV-O)	Forward	5′-GGAATTCCCACCATGAG CACGAATCCTAAACCTC-3
	Reverse	5′-ATAAGAATGCGGCCGCC TATCAAGCGGAAGCTGG GATGGT-3′
pcDNA3/core(HCV-O)	Forward	5′-CGGGATCCAAGATGAGC ACGAATCCTAAACCTCAA AGA-3′
pcDNA3/FLAG-core(HCV-O)	Reverse	5′-CCGCTCGAGTCAAGCGG AAGCTGGGATGGTCAAA CA-3′
pcDNA3/Δcore(HCV-O)	Forward	5′-CGGGATCCAAGATGGGC CCCAGGTTGGGTGTGCG C-3′
pcDNA3/FLAG-Δcore(HCV-O)	Reverse	5′-CCGCTCGAGTCAAGCGG AAGCTGGGATGGTCAAA CA-3′
pcDNA3/core(JFH1)	Forward	5′-CGGGATCCAAGATGAGC ACAAATCCTAAACCTCAA AGA-3′
pcDNA3/FLAG-core(JFH1)	Reverse	5′-CCGCTCGAGTCAAGCAG AGACCGGAACGGTGATG CA-3′
pcDNA3/Δcore(JFH1)	Forward	5′-CGGGATCCAAGATGGGC CCCAGGTTGGGTGTGCG C-3′
pcDNA3/FLAG-Δcore(JFH1)	Reverse	5′-CCGCTCGAGTCAAGCAG AGACCGGAACGGTGATG CA-3′

[a] To construct pCXbsr/core(HCV-O), a DNA fragment encoding the core was amplified by PCR from pON/C-5B (13) with the indicated primers. The PCR product was digested with EcoRI-NotI and subcloned into the same site of pCX4bsr (1). To construct pcDNA3/core(HCV-O), pcDNA3/FLAG-core(HCV-O), pcDNA3/Δcore(HCV-O), and pcDNA3/FLAG-Δcore(HCV-O), DNA fragments encoding the core were amplified by PCR from pON/C-5B (13) with the indicated primer sets. To construct pcDNA3/core(JFH1), pcDNA3/FLAG-core(JFH1), pcDNA3/Δcore(JFH1), and pcDNA3/FLAG-Δcore(JFH1), DNA fragments encoding the core were amplified by PCR from pJFH1 (23) with the indicated primer sets. The PCR products were digested with BamHI and XhoI and then subcloned into the same site of pcDNA3 (Invitrogen) or pcDNA3-FLAG (2).

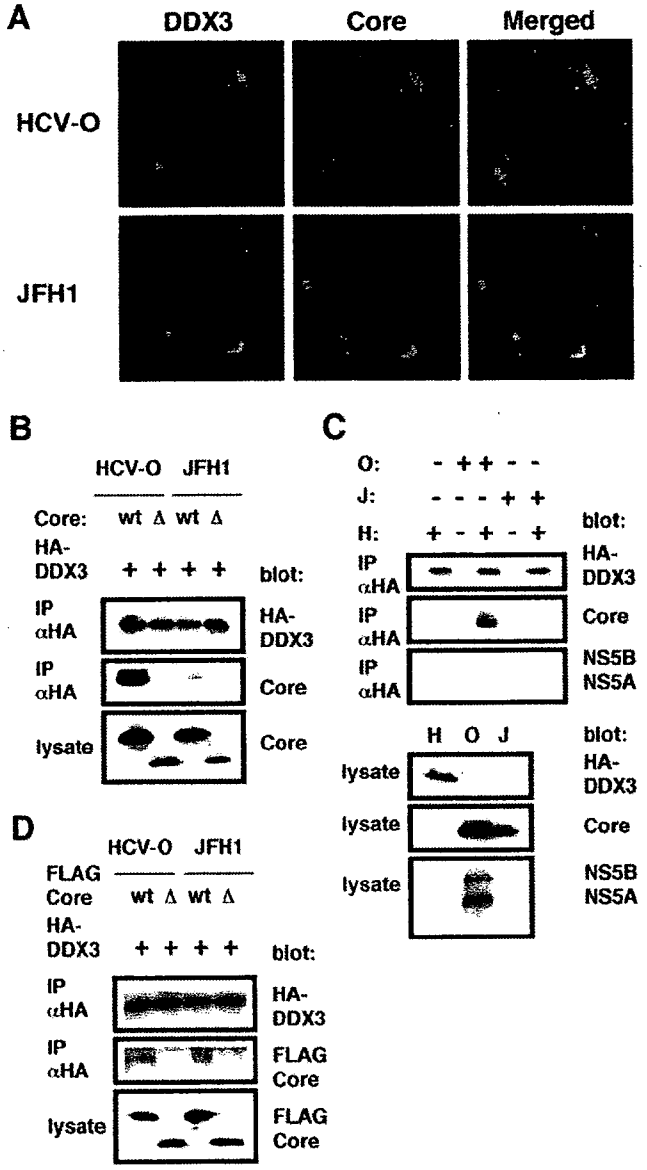

FIG. 2. Interaction of the HCV core with DDX3. (A) The HCV core colocalizes with DDX3. 293FT cells cotransfected with 100 ng of pCXbsr/core(HCV-O) or pcDNA3/core(JFH1) and 200 ng of pHA-DDX3 were examined by confocal laser scanning microscopy. Cells were stained with anti-HCV core (CP-9 and CP-11 mixture) and anti-DDX3 antibodies and were then visualized with fluorescein isothiocyanate (DDX3) or Cy3 (core). Images were visualized using confocal laser scanning microscopy (LSM510; Carl Zeiss). The right panels exhibit the two-color overlay images (Merged). Colocalization is shown in yellow. (B) The core binds to DDX3. 293FT cells were cotransfected with 4 μg of pHA-DDX3 and 4 μg of pCXbsr/core(HCV-O) (wt), pcDNA3/Δcore(HCV-O) (Δ), pcDNA3/core(JFH1) (wt), or pcDNA3/Δcore(JFH1) (Δ). The cell lysates were immunoprecipitated with an anti-HA antibody (3F10; Roche), followed by immunoblot analysis using either anti-HA (HA-7; Sigma) or anti-HCV core antibody (CP-9 and CP-11 mixture). (C) 293FT cells transfected with 4 μg of pHA-DDX3 (H), O cells (O), or RSc cells 3 days after inoculation of HCVcc (JFH1) (J) were lysed and immunoprecipitated (IP) with 1 μg of anti-HA antibody (3F10), followed by immunoblotting with anti-HA (HA-7), anti-core (CP-9 and CP-11 mixture), or anti-HCV NS5A (no. 8926) and anti-HCV NS5B. (D) 293FT cells transfected with 4 μg of pHA-DDX3 and 4 μg of pcDNA3/FLAG-core(HCV-O) (wt), pcDNA3/FLAG-Δcore(HCV-O) (Δ), pcDNA3/FLAG-core(JFH1) (wt), or pcDNA3/FLAG-Δcore(JFH1) (Δ) were lysed and immunoprecipitated with 1 μg of an anti-HA antibody (3F10), followed by immunoblotting with an anti-HA (HA-7) or anti-core (CP-9 and CP-11 mixture) antibody.

on 30 μl of protein G-Sepharose resin for 1 h, the resin was washed four times with 700 μl lysis buffer. Proteins were eluted by boiling the resin for 5 min in 1× Laemmli sample buffer. The proteins were then subjected to sodium dodecyl sulfate-polyacrylamide gel electrophoresis, followed by immunoblot analysis using either anti-HA (HA-7; Sigma) or anti-HCV core antibody (CP-9 and CP-11 mixture). We observed that the HCV-O core but not its N-truncated mutant could strongly bind to HA-tagged DDX3 (Fig. 2B). In contrast, the binding activity of the JFH1 core to HA-tagged DDX3 seemed to be fairly weak (Fig. 2B). As well, immunoprecipitation of lysates of 293FT cells expressing HA-tagged DDX3, O cells, or JFH1-infected RSc cells, or mixtures of these lysates, with an anti-HA antibody revealed that HCV-O core but not JFH1 core could bind strongly to DDX3 (Fig. 2C). The anti-HCV core antibody we used could detect both HCV-O core and JFH1 core (Fig. 2), while both anti-HCV NS5A and anti-NS5B antibodies failed to detect JFH1 NS5A and NS5B (Fig. 2C). At least, we failed to detect an interaction between DDX3 and either HCV-O NS5A or NS5B under experimental conditions that permitted the core to interact with DDX3 by immunoprecipitation (Fig. 2C). In contrast, the FLAG-tagged JFH1 core could bind to HA-tagged DDX3 just as efficiently as the FLAG-tagged HCV-O core could (Fig. 2D). Thus, the binding affinity or stability of the complex formed between the JFH1 core and DDX3 might be weaker than that between the HCV-O core and DDX3.

Since DDX3 is required for HIV-1 and HCV replication, we hypothesized that the HCV core might affect the function of HIV-1 Rev when both proteins were coexpressed. To test this hypothesis, we used the Rev-dependent luciferase-based reporter plasmid pDM628, harboring a single intron that includes both the Rev-responsive element (RRE) and the luciferase coding sequences (Fig. 3A) (10). In this system, Rev binds to RRE on the unspliced reporter mRNA, allowing its export from the nucleus for luciferase reporter gene expression, while the intron containing the luciferase gene is excised during RNA splicing when cells are transiently transfected with pDM628 alone. As previously reported (10), the luciferase activity in 293FT cells transfected with this reporter plasmid was stimulated by Rev, which induced a fourfold increase in the reporter signal (Fig. 3B). Luciferase activity was increased eightfold by the combination of Rev and DDX3, whereas neither the HCV-O core nor the JFH1 core had any effect on this Rev function (Fig. 3B). Since the Rev-binding domain (the N-terminal domain) and the core-binding domain (the C-terminal domain) do not overlap in DDX3, the HCV core might not compete with HIV-1 Rev for binding with DDX3. However, the development of a novel DDX3 inhibitor might provide a powerful antiviral agent against both HIV-1 and HCV (15).

Taking these results together, this study has shown for the first time that DDX3 is required for HCV RNA replication.

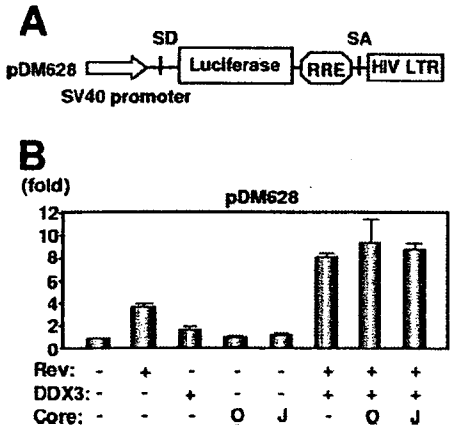

FIG. 3. HCV core does not affect the DDX3-mediated synergistic activation of Rev function. (A) Schematic representation of HIV-1 Rev-dependent luciferase-based reporter plasmid pDM628 harboring a splicing donor (SD), splicing acceptor (SA), and RRE. (B) 293FT cells were cotransfected with 100 ng of pDM628, 200 ng of pcRev, 200 ng of pHA-DDX3, and/or 100 ng of either pcDNA3/core(HCV-O) (O) or pcDNA3/core(JFH1) (J). A luciferase assay was performed 24 h later. All transfections utilized equal total amounts of plasmid DNA owing to the addition of the empty vector pcDNA3 to the transfection mixture. The relative stimulation of luciferase activity (*n*-fold) is shown. The results shown are means from three independent experiments.

Since helicases are motor enzymes that use energy derived from nucleoside triphosphate hydrolysis to unwind double-stranded nucleic acids, the DDX3–core complex might unwind the HCV double-stranded RNA and separate the RNA strands or might contribute to the function of HCV NS3 helicase. Since the replication of subgenomic replicon RNA was also partially suppressed in DDX3 knockdown cells (Fig. 1D), DDX3 might be associated with an HCV nonstructural protein(s) or HCV RNA itself. Indeed, Tingting et al. recently reported that DDX1 bound to both the HCV 3′ untranslated region (3′ UTR) and the HCV 5′ UTR and that short interfering RNA-mediated knockdown of DDX1 caused a marked reduction in the replication of subgenomic replicon RNA (22). Furthermore, Goh et al. demonstrated that DDX5/p68 associated with HCV NS5B and that depletion of endogenous DDX5 correlated with a reduction in the transcription of negative-strand HCV RNA (11). However, we failed to observe an interaction between DDX3 and NS5A or NS5B by immunoprecipitation under our experimental conditions in which the core could interact with DDX3 (Fig. 2C). Importantly, our DDX3 knockdown study demonstrated a more significant reduction in the accumulation of genome-length HCV RNA (95% reduction) than in the accumulation of subgenomic replicon RNA (52% reduction) (Fig. 1B and D). To date, it has been demonstrated that the 5′ UTR, the 3′ UTR, and the NS3-to-NS5B coding region are sufficient for HCV RNA replication (16); however, the core might be partly involved in the replication of genome-length HCV RNA. Importantly, DDX1 and DDX3 were specifically detected in the lipid droplets of core-expressing Hep39 cells by proteomic analysis (21), suggesting that DDX3 might be associated with HCV assembly or might incorporate into the HCV virion through interaction with the core to act as an RNA chaperone.

Recent studies have suggested a potential role of DDX3 and DDX5 in the pathogenesis of HCV-related liver diseases. DDX3 expression is deregulated in HCV-associated HCC (7, 8), and Huang et al. identified single-nucleotide polymorphisms in the DDX5 gene that were significantly associated with an increased risk of advanced fibrosis in patients with chronic hepatitis C (12). Interestingly, DDX3 might be a candidate tumor suppressor. DDX3 inhibits colony formation in various cell lines, including HuH-7, and up-regulates the $p21^{waf1/cip1}$ promoter (8). If DDX3 could in fact suppress tumor growth, then the core might overcome DDX3-mediated cell growth arrest and down-regulate $p21^{waf1/cip1}$ through interaction with DDX3, and it might also be involved in HCC development.

We thank D. Trono, K.-T. Jeang, V. Yedavalli, R. J. Pomerantz, J. Fang, R. Iggo, M. Hijikata, T. Akagi, and M. Kohara for pCMVΔR8.91, pMDG2, pHA-DDX3, pDM628, pcRev, pSUPER, pRDI292, 293FT cells, pCX4bsr, and the anti-NS5B antibody. We also thank A. Morishita and T. Nakamura for technical assistance.

This work was supported by a Grant-in-Aid for Young Scientists (B) from the Ministry of Education, Culture, Sports, Science, and Technology (MEXT), by a Grant-in-Aid for Research on Hepatitis from the Ministry of Health, Labor, and Welfare of Japan, by the Naito Foundation, by the Ichiro Kanehara foundation, and by a research fellowship from the Japan Society for the Promotion of Science (JSPS).

REFERENCES

1. **Akagi, T., T. Shishido, K. Murata, and H. Hanafusa.** 2000. v-Crk activates the phosphoinositide 3-kinase/AKT pathway in transformation. Proc. Natl. Acad. Sci. USA **97**:7290–7295.
2. **Ariumi, Y., A. Kaida, M. Hatanaka, and K. Shimotohno.** 2001. Functional cross-talk of HIV-1 Tat with p53 through its C-terminal domain. Biochem. Biophys. Res. Commun. **287**:556–561.
3. **Ariumi, Y., T. Ego, A. Kaida, M. Matsumoto, P. P. Pandolfi, and K. Shimotohno.** 2003. Distinct nuclear body components, PML and SMRT, regulate the *trans*-acting function of HTLV-1 Tax oncoprotein. Oncogene **22**:1611–1619.
4. **Ariumi, Y., P. Turelli, M. Masutani, and D. Trono.** 2005. DNA damage sensors ATM, ATR, DNA-PKcs, and PARP-1 are dispensable for human immunodeficiency virus type 1 integration. J. Virol. **79**:2973–2978.
5. **Bridge, A. J., S. Pebernard, A. Ducraux, A.-L. Nicoulaz, and R. Iggo.** 2003. Induction of an interferon response by RNAi vectors in mammalian cells. Nat. Genet. **34**:263–264.
6. **Brummelkamp, T. R., R. Bernard, and R. Agami.** 2002. A system for stable expression of short interfering RNAs in mammalian cells. Science **296**:550–553.
7. **Chang, P. C., C. W. Chi, G. Y. Chau, F. Y. Li, Y. H. Tsai, J. C. Wu, and Y. H. Lee.** 2006. DDX3, a DEAD box RNA helicase, is deregulated in hepatitis virus-associated hepatocellular carcinoma and is involved in cell growth control. Oncogene **25**:1991–2003.
8. **Chao, C. H., C. M. Chen, P. L. Cheng, J. W. Shih, A. P. Tsou, and Y. H. Lee.** 2006. DDX3, a DEAD box RNA helicase with tumor growth-suppressive property and transcriptional regulation activity of the $p21^{waf1/cip1}$ promoter, is a candidate tumor suppressor. Cancer Res. **66**:6579–6588.
9. **Cordin, O., J. Banroques, N. K. Tanner, and P. Linder.** 2006. The DEAD-box protein family of RNA helicases. Gene **367**:17–37.
10. **Fang, J., S. Kubota, B. Yang, N. Zhou, H. Zang, R. Godbout, and R. J. Pomerantz.** 2004. A DEAD box protein facilitates HIV-1 replication as a cellular co-factor of Rev. Virology **330**:471–480.
11. **Goh, P. Y., Y. J. Tan, S. P. Lim, Y. H. Tan, S. G. Lim, F. Fuller-Pace, and W. Hong.** 2004. Cellular RNA helicase p68 relocalization and interaction with the hepatitis C virus (HCV) NS5B protein and the potential role of p68 in HCV RNA replication. J. Virol. **78**:5288–5298.
12. **Huang, H., M. L. Shiffman, R. C. Cheung, T. J. Layden, S. Friedman, O. T. Abar, L. Yee, A. P. Chokkalingam, S. J. Schrodi, J. Chan, J. J. Catanese, D. U. Leong, D. Ross, X. Hu, A. Monto, L. B. McAllister, S. Broder, T. White, J. J. Sninsky, and T. L. Wright.** 2006. Identification of two gene variants associated with risk of advanced fibrosis in patients with chronic hepatitis C. Gastroenterology **130**:1679–1687.
13. **Ikeda, M., K. Abe, H. Dansako, T. Nakamura, K. Naka, and N. Kato.** 2005. Efficient replication of a full-length hepatitis C virus genome, strain O, in cell culture, and development of a luciferase reporter system. Biochem. Biophys. Res. Commun. **329**:1350–1359.
14. **Kato, N., K. Sugiyama, K. Namba, H. Dansako, T. Nakamura, M. Takami,**

K. Naka, A. Nozaki, and K. Shimotohno. 2003. Establishment of a hepatitis C virus subgenomic replicon derived from human hepatocytes infected in vitro. Biochem. Biophys. Res. Commun. **306**:756–766.
15. **Kwong, A. D., B. G. Rao, and K. T. Jeang.** 2005. Viral and cellular RNA helicases as antiviral targets. Nat. Rev. Drug Discov. **4**:845–853.
16. **Lohmann, V., F. Körner, J.-O. Koch, U. Herian, L. Theilman, and R. Bartenschlager.** 1999. Replication of subgenomic hepatitis C virus RNAs in a hepatoma cell line. Science **285**:110–113.
17. **Mamiya, N., and H. J. Worman.** 1999. Hepatitis C virus core protein binds to a DEAD box RNA helicase. J. Biol. Chem. **274**:15751–15756.
18. **Naldini, L., U. Blömer, P. Gallay, D. Ory, R. Mulligan, F. H. Gage, I. M. Verma, and D. Trono.** 1996. In vivo gene delivery and stable transduction of non-dividing cells by a lentiviral vector. Science **272**:263–267.
19. **Owsianka, A. M., and A. H. Patel.** 1999. Hepatitis C virus core protein interacts with a human DEAD box protein DDX3. Virology **257**:330–340.
20. **Rocak, S., and P. Linder.** 2004. DEAD-box proteins: the driving forces behind RNA metabolism. Nat. Rev. Mol. Cell Biol. **5**:232–241.
21. **Sato, S., M. Fukasawa, Y. Yamakawa, T. Natsume, T. Suzuki, I. Shoji, H. Aizaki, T. Miyamura, and M. Nishijima.** 2006. Proteomic profiling of lipid droplet proteins in hepatoma cell lines expressing hepatitis C virus core protein. J. Biochem. **139**:921–930.
22. **Tingting, P., F. Caiyun, Y. Zhigang, Y. Pengyuan, and Y. Zhenghong.** 2006. Subproteomic analysis of the cellular proteins associated with the 3′ untranslated region of the hepatitis C virus genome in human liver cells. Biochem. Biophys. Res. Commun. **347**:683–691.
23. **Wakita, T., T. Pietschmann, T. Kato, T. Date, M. Miyamoto, Z. Zhao, K. Murthy, A. Habermann, H. G. Kräusslich, M. Mizokami, R. Bartenschlager, and T. J. Liang.** 2005. Production of infectious hepatitis C virus in tissue culture from a cloned viral genome. Nat. Med. **11**:791–796.
24. **Yedavalli, V. S., C. Neuveut, Y. H. Chi, L. Kleiman, and K. T. Jeang.** 2004. Requirement of DDX3 DEAD box RNA helicase for HIV-1 Rev-RRE export function. Cell **119**:381–392.
25. **Yon, L. R., C. M. Chen, T. S. Yeh, T. Y. Tsai, R. T. Mai, C. H. Lin, and Y. H. Lee.** 1999. Hepatitis C virus core protein interacts with cellular putative RNA helicase. J. Virol. **73**:2841–2853.
26. **Zufferey, R., D. Nagy, R. J. Mandel, L. Naldini, and D. Trono.** 1997. Multiply attenuated lentiviral vector achieves efficient gene delivery in vivo. Nat. Biotechnol. **15**:871–875.

nature
cell biology

The lipid droplet is an important organelle for hepatitis C virus production

Yusuke Miyanari[1,2], Kimie Atsuzawa[3], Nobuteru Usuda[3], Koichi Watashi[1,2], Takayuki Hishiki[1,2], Margarita Zayas[4], Ralf Bartenschlager[4], Takaji Wakita[5], Makoto Hijikata[1,2] and Kunitada Shimotohno[1,2,6]

The lipid droplet (LD) is an organelle that is used for the storage of neutral lipids. It dynamically moves through the cytoplasm, interacting with other organelles, including the endoplasmic reticulum (ER)[1–3]. These interactions are thought to facilitate the transport of lipids and proteins to other organelles. The hepatitis C virus (HCV) is a causative agent of chronic liver diseases[4]. HCV capsid protein (Core) associates with the LD[5], envelope proteins E1 and E2 reside in the ER lumen[6], and the viral replicase is assumed to localize on ER-derived membranes. How and where HCV particles are assembled, however, is poorly understood. Here, we show that the LD is involved in the production of infectious virus particles. We demonstrate that Core recruits nonstructural (NS) proteins and replication complexes to LD-associated membranes, and that this recruitment is critical for producing infectious viruses. Furthermore, virus particles were observed in close proximity to LDs, indicating that some steps of virus assembly take place around LDs. This study reveals a novel function of LDs in the assembly of infectious HCV and provides a new perspective on how viruses usurp cellular functions.

Hepatitis C virus (HCV) has a plus-strand RNA genome that encodes the viral structural proteins Core, E1 and E2, the p7, and the nonstructural (NS) proteins 2, 3, 4A, 4B, 5A and 5B (refs 7, 8). NS proteins are reported to localize on the cytoplasmic side of endoplasmic reticulum (ER) membranes[9]. To elucidate the mechanisms of virus production, we used a HCV strain, JFH1, which can produce infectious viruses[10–12]. We first investigated the subcellular localization of the HCV proteins in cells that had been transfected with JFH1^{E2FL} RNA, in which a part of the hypervariable region 1 of E2 was replaced by the FLAG epitope tag (see Supplementary Information, Fig. S1, S2a–d). Core localized to the lipid droplets (LDs; Fig. 1a), as previously reported[5]. Interestingly, NS proteins were also detected around LDs in 60–90% of JFH1^{E2FL}-replicating cells (Fig. 1a, c). Similar levels of colocalization of LDs with viral proteins were observed in cells that had been transfected with chimeric HCV genomes expressing structural proteins, p7 and part of NS2 of the genotype 1b (Con1) or the genotype 1a (H77) isolate (see Supplementary Information, Fig. S1, S2e)[13]. In contrast, there was no close association between the LDs and NS proteins in cells that had been transfected with JFH1^{dC3} RNA (Fig. 1b, c), which lacked the coding region of Core (Supplementary Information, Fig. S1). NS proteins were diffusely present on the ER, suggesting that NS proteins are translocated from the ER to LDs in JFH1^{E2FL}-replicating cells in a Core-dependent manner. Importantly, there was no association between LDs and PDI, an ER marker protein, indicating that either ER membranes were absent in close proximity to LDs or that PDI was excluded from such membranes (Fig. 1c). These results were supported by western blot analysis of the LD fraction (Fig. 1d). The LD fraction contained ADRP, an LD marker, but not the ER markers Calnexin and Grp78 (data not shown), indicating that there was no ER contamination in the LD fraction. However, the LD fraction from JFH1^{E2FL}-replicating cells contained high levels of viral proteins in contrast to the LD fraction from JFH1^{dC3}-replicating cells (in which HCV proteins were virtually absent (Fig. 1d, LD fraction)), even though the expression levels of the NS proteins in whole-cell extracts were similar (Fig. 1d, whole-cell extract). About 20–45% of the total HCV proteins associated with the LDs in JFH1^{E2FL}-replicating cells (Fig. 1e). Consistent with previous reports that Core enhances the formation of LDs[14], overproduction of LDs was observed in JFH1^{E2FL}-, but not JFH1^{dC3}-replicating cells (Supplementary Information, Fig. S3a–l). Treatment of the cells with oleic acid, which enhanced the formation of LDs, did not affect either HCV protein levels or the recruitment of viral proteins to LDs in JFH1^{dC3}-replicating cells (Supplementary Information, Fig. S3m–p). Thus, the overproduction of LDs is insufficient for the recruitment of HCV proteins to LDs. To examine the ability of Core to recruit NS proteins to LDs, JFH1^{dC3}-replicating cells were transfected with a plasmid-expressing Core (Core^{WT}) (Fig. 1f, g). NS5A accumulated around LDs (Fig. 1f, arrowheads and panel 2), as did NS3 and NS4AB (Fig. 1g), in cells expressing Core^{WT}. The translocation of NS proteins to LDs was, however, not observed in JFH1^{dC3}-replicating cells expressing Core$^{PP/AA}$ (Fig. 1g and Supplementary Information, Fig. S2f–h),

[1]Department of Viral Oncology, Institute for Virus Research, Kyoto University, Kyoto 606-8507, Japan; [2]Graduate School of Biostudies, Kyoto University, Kyoto 606-8507, Japan; [3]Department of Anatomy, Fujita Health University School of Medicine, Toyoake 470-1192, Japan; [4]Department of Molecular Virology, University of Heidelberg, 69120 Heidelberg, Germany; [5]Department of Virology II, National Institute of Infectious Diseases, Tokyo 162-8640, Japan
[6]Correspondence should be addressed to K.S. (e-mail: shimkuni@z8.keio.jp)

Received 16 March 2007; accepted 31 July 2007; published online 26 August 2007; DOI: 10.1038/ncb1631

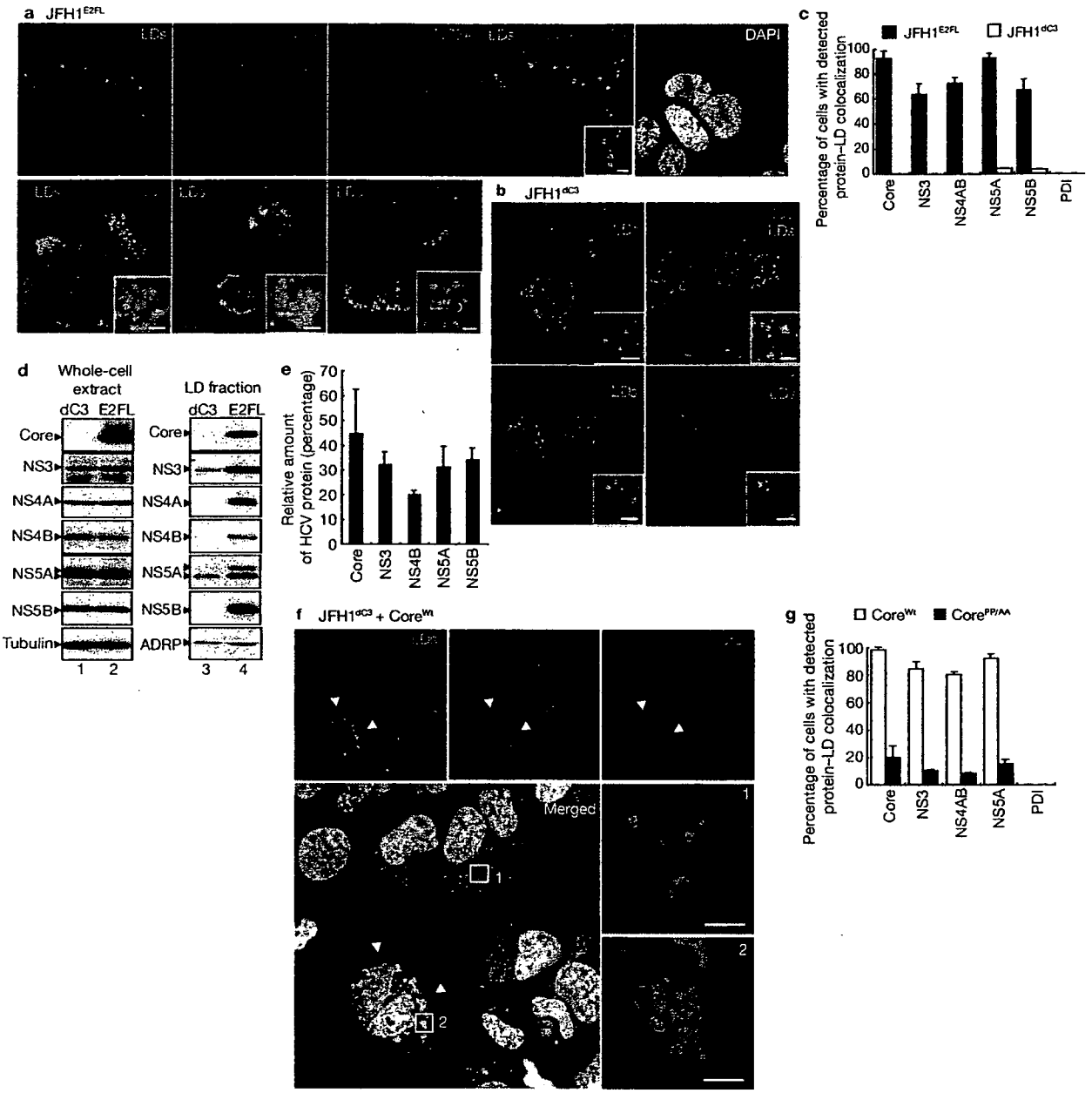

Figure 1 Core recruits NS proteins to LDs. (a) Huh-7 cells transfected with JFH1^{E2FL} RNA were labelled with antibodies against Core (red), NS5A (blue), NS3 (red), NS4AB (red) or NS5B (red). Lipid droplets (LDs) and nuclei were stained with BODYPI 493/503 (green) and DAPI (white in upper panel, blue in lower panels), respectively. Insets are high magnification images of areas in the respective panel. (b) JFH1^{dC3} replicon-bearing cells were labelled with DAPI (blue), BODIPY 493/503 (green) and indicated antibodies (red). The insets are high magnifications of the corresponding panel. (c) Percentages of JFH1^{E2FL}- or JFH1^{dC3}-bearing cells in which hepatitis C virus (HCV) proteins or PDI colocalize with LDs ($n > 200$). (d) Western blot analysis of HCV proteins and marker proteins in whole-cell extracts and the LD fractions from cells transfected with JFH1^{E2FL} (E2FL) or JFH1^{dC3} (dC3) RNA. (e) HCV proteins were quantified by using western blotting data of the purified LD fraction and whole-cell extracts of JFH1^{E2FL}-replicating cells. Results are shown as relative amounts of HCV proteins co-fractionated with LDs. This results correspond well with results obtained by quantitative immunofluorescence staining (data not shown). (f) Trans-complementation with Core^{Wt} relocates NS proteins to LDs. JFH1^{dC3} replicon-bearing cells were transfected with pcDNA3–Core^{Wt} and labelled with BODIPY 493/503 (green), DAPI (white) and antibodies against NS5A (red) and Core (blue). Arrowheads indicate Core^{Wt}-expressing cells. Higher-magnification images of area 1 and area 2 are shown in panels 1 and 2, respectively. Scale bars, 2 μm. (g) The percentages of cells in which HCV proteins colocalize with LDs in the presence of Core^{Wt} or Core $^{PP/AA}$ ($n > 200$). Uncropped images of gels are shown in Supplementary Information Fig. S6. All error bars are derived from s.d.

a variant of Core containing two alanine substitutions at amino-acid positions 138 and 143 that fails to associate with LDs[15]. These results show that LD-associated Core recruits NS proteins from the ER to LDs.

Next, we investigated whether Core also recruited HCV RNA to LDs. *In situ* hybridization analysis showed that in more than 80% of JFH1^{E2FL}-replicating cells, both plus- and minus-strand RNAs were diffusely

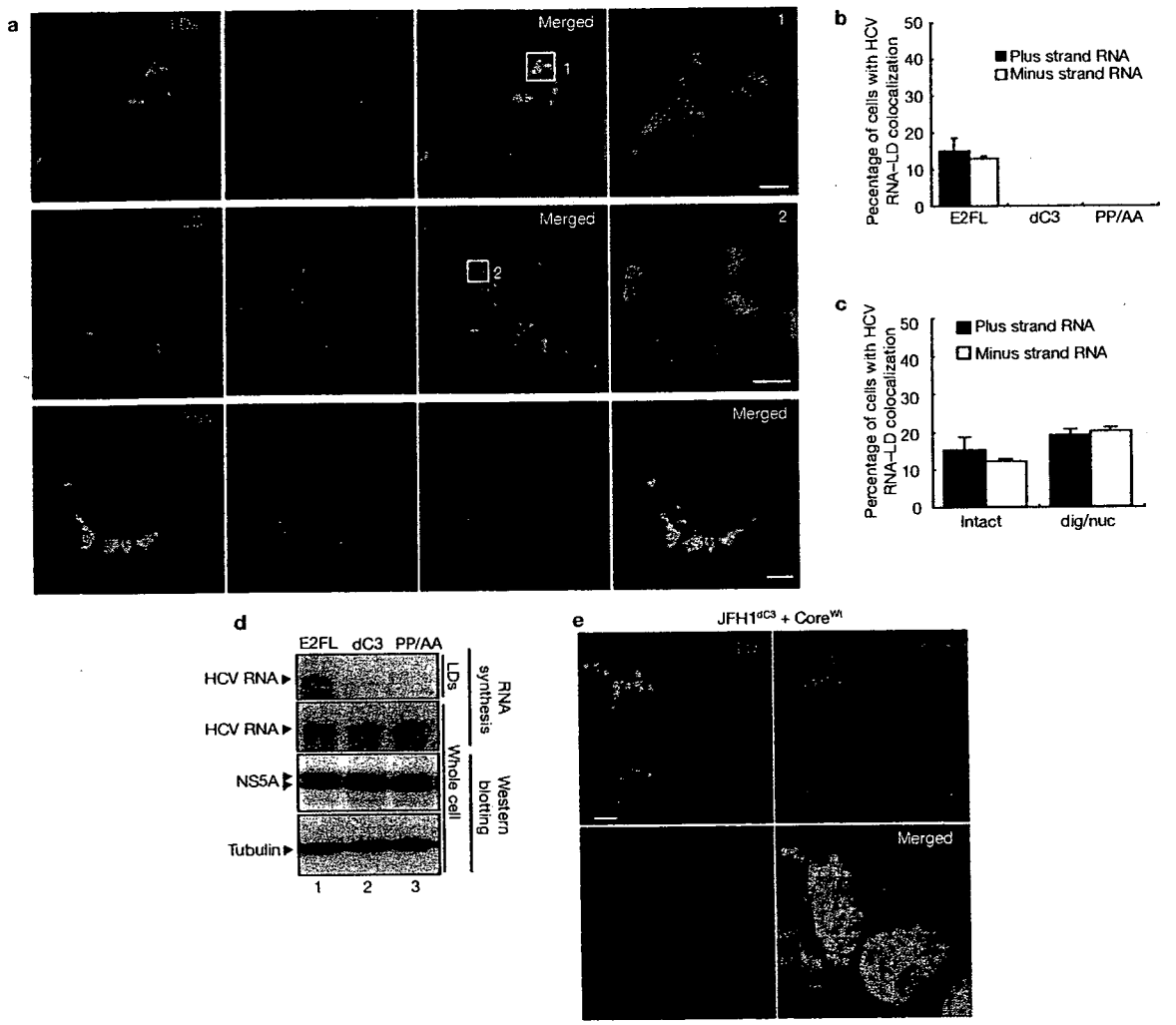

Figure 2 Core-dependent recruitment of active HCV replication complexes to the LD. (**a**) Huh-7 cells transfected with JFH1^{E2FL} RNA were analysed by *in situ* hybridization with strand-specific probes (plus or minus). The cells were labelled to simultaneously visualize lipid droplets (LDs), NS5A and Core (lower panels). Higher-magnification images of area 1 and area 2 are shown in the upper and middle right panels 1 and 2, respectively. Scale bars: 2 μm (panels 1, 2); 10 μm (lower right panel). (**b**) The percentages of JFH1^{E2FL}-, JFH1^{dC3}- and JFH1$^{PP/AA}$-expressing cells positive for overlapping signals for LDs and plus- or minus-strand hepatitis C virus (HCV) RNA ($n > 200$). (**c**) Intact or digitonin and nuclease-treated (dig/nuc) JFH1^{E2FL} replicon-bearing cells were analysed by *in situ* hybridization. The percentages of cells with overlapping signals for LD and plus- or minus-strand HCV RNA are shown ($n > 200$). (**d**) RNA-synthesizing activity in the LD fractions purified from cells transfected with JFH1^{E2FL}, JFH1^{dC3} or JFH1$^{PP/AA}$ RNA (top panel). As a control, HCV RNA synthesis activity in digitonin-permeabilized cells was analysed (second panel from the top). HCV protein levels represented by NS5A are shown, together with the level of tubulin (bottom two panels). (**e**) Localization of plus-strand HCV RNA and Core in JFH1^{dC3} replicon-bearing cells transfected with pcDNA3–Core^{Wt} (Scale bar, 10 μm). Uncropped images of gels are shown in Supplementary Information Fig. S6. All error bars are derived from s.d.

located in the perinuclear region (see Supplementary Information, Fig. S4a). More importantly, in about 20% of these cells, plus- and minus-strand RNAs accumulated around LDs (Fig. 2a, upper and middle panels; 2b) and colocalized with HCV proteins such as Core and NS5A (Fig. 2a, lower panels). No association between HCV RNA and LDs was detected in JFH1^{dC3}- or JFH1$^{PP/AA}$-replicating cells (Fig. 2b). Northern blot analysis revealed that 4.8% and 5.4% of total plus- and minus-strand HCV RNA, respectively, were detected in purified LD fractions of JFH^{E2FL}-replicating cells (data not shown). Induction of LD formation with oleic acid did not affect HCV RNA accumulation around LDs (data not shown). These results provide strong evidence that Core recruits HCV RNA as well as NS proteins to LDs.

The HCV replication complex is compartmentalized by lipid bilayer membranes[16–18]. Therefore, HCV RNA in the complex is resistant to nuclease treatment in digitonin-permeabilized cells[17] (Supplementary Information, Fig. S4b–d). *In situ* hybridization analysis did not reveal a significant difference in the number of cells containing LD-associated HCV RNA before and after nuclease treatment (Fig. 2c), indicating that HCV RNA around LDs is part of the replication complex. An RNA synthesis assay showed that the purified LD fraction from JFH1^{E2FL}-, but not JFH1^{dC3}- or JFH1$^{PP/AA}$-replicating cells, possessed HCV RNA synthesis activity, even though the expression levels of viral proteins and RNA-synthesizing activities in total cell lysates were similar (Fig. 2d). Moreover, the addition of Core^{Wt} rescued the localization of plus- and minus-strand

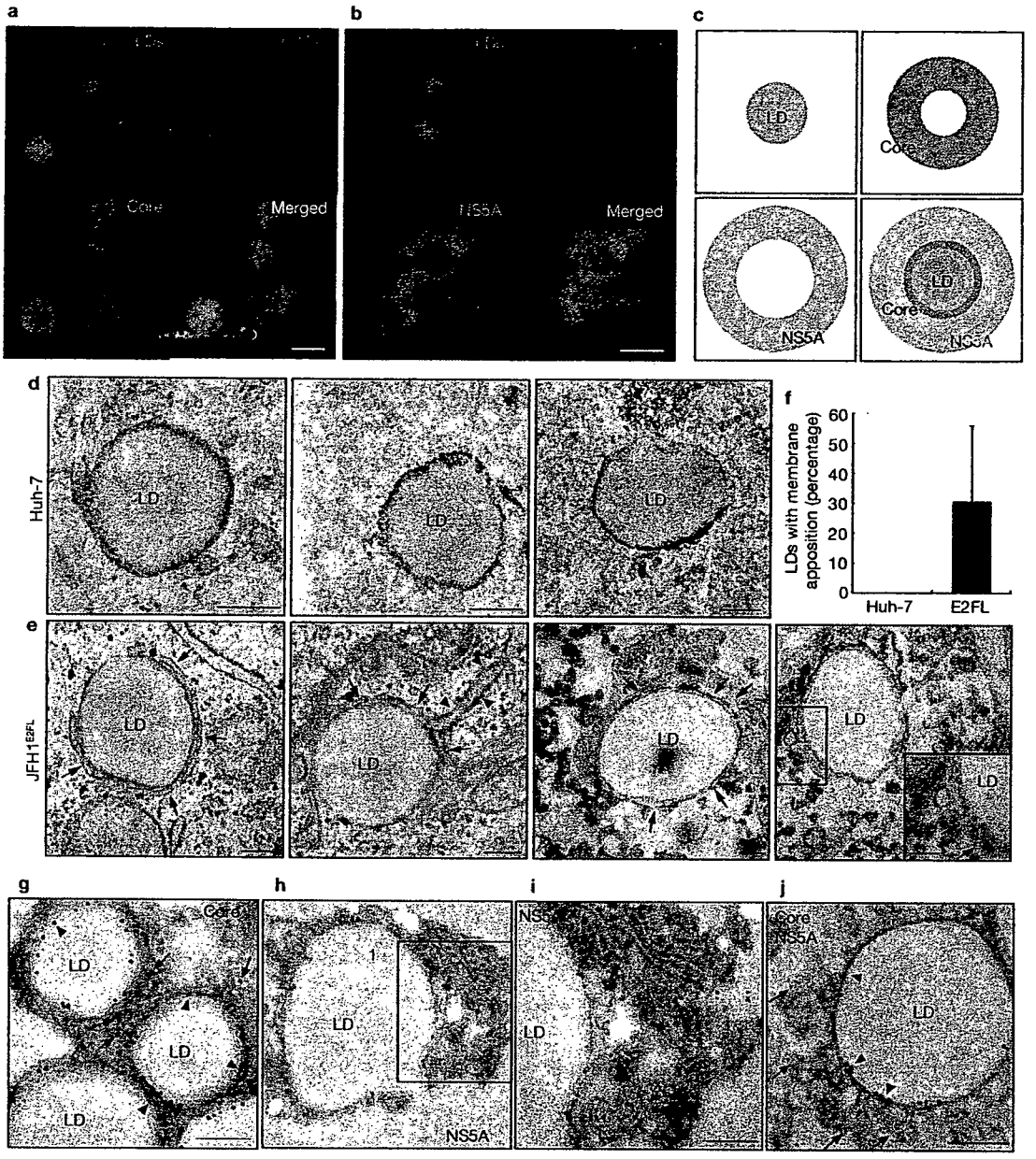

Figure 3 Spatial distribution of Core and NS5A relative to the LD. (**a**, **b**) The localizations of Core, NS5A and ADRP around the lipid droplets (LDs) in JFH1^{E2FL} replicon-bearing cells were analysed using immunofluorescence microscopy. Scale bars, 1 μm. (**c**) Typical images of the localization of LDs, Core, NS5A and merged images are shown with the relative scale of each image. (**d**, **e**) Transmission electron micrographs of LDs in naïve Huh-7 cells and JFH1^{E2FL}-expressing cells. Arrows and arrowheads indicate LD-associated membranes and rough ER membranes, respectively. (**f**) Frequency of LDs with close appositions of membrane cisternae. About 100 Huh-7 cells or JFH1^{E2FL}-expressing cells, respectively, were chosen randomly. LDs with apposed membrane cisternae, as exemplified in panel **e**, were counted as positive. The LDs judged as positive were divided by the total number of LDs. (**g**–**j**) Immunoelectron micrographs of LDs labelled with antibodies against Core (**g**), NS5A (**h**, **i**) or both (**j**) are shown. Panel **i** is a higher magnification of area 1 in panel **h**. In panel **j**, Core and NS5A are labelled with 15 nm and 10 nm gold particles, respectively. Scale bars, 200 nm. All error bars are derived from s.d.

HCV RNA around LDs in JFH^{dC3}-replicating cells (Fig. 2e and data not shown). Both plus- and minus-strand RNA associated with LDs were nuclease resistant (data not shown). These results demonstrate that Core recruits biologically active replication complexes to LDs.

The LD is surrounded by a phospholipid monolayer[19], whereas HCV replication complexes are likely to be surrounded by lipid bilayer membranes[16,17]. Therefore, the replication complexes might not be directly associated with the membranes of LDs. To characterize the colocalization of LDs, viral proteins and replication complexes more precisely, we analysed the localization of NS5A with high-resolution immunofluorescence microscopy. Core was completely colocalized with ADRP, residing on the surface of LDs[20] (Fig. 3a), thus indicating that Core also directly associates with the surface of LDs. More importantly, NS5A mainly localized around the Core-positive area, resulting in a doughnut-shaped signal with a diameter slightly

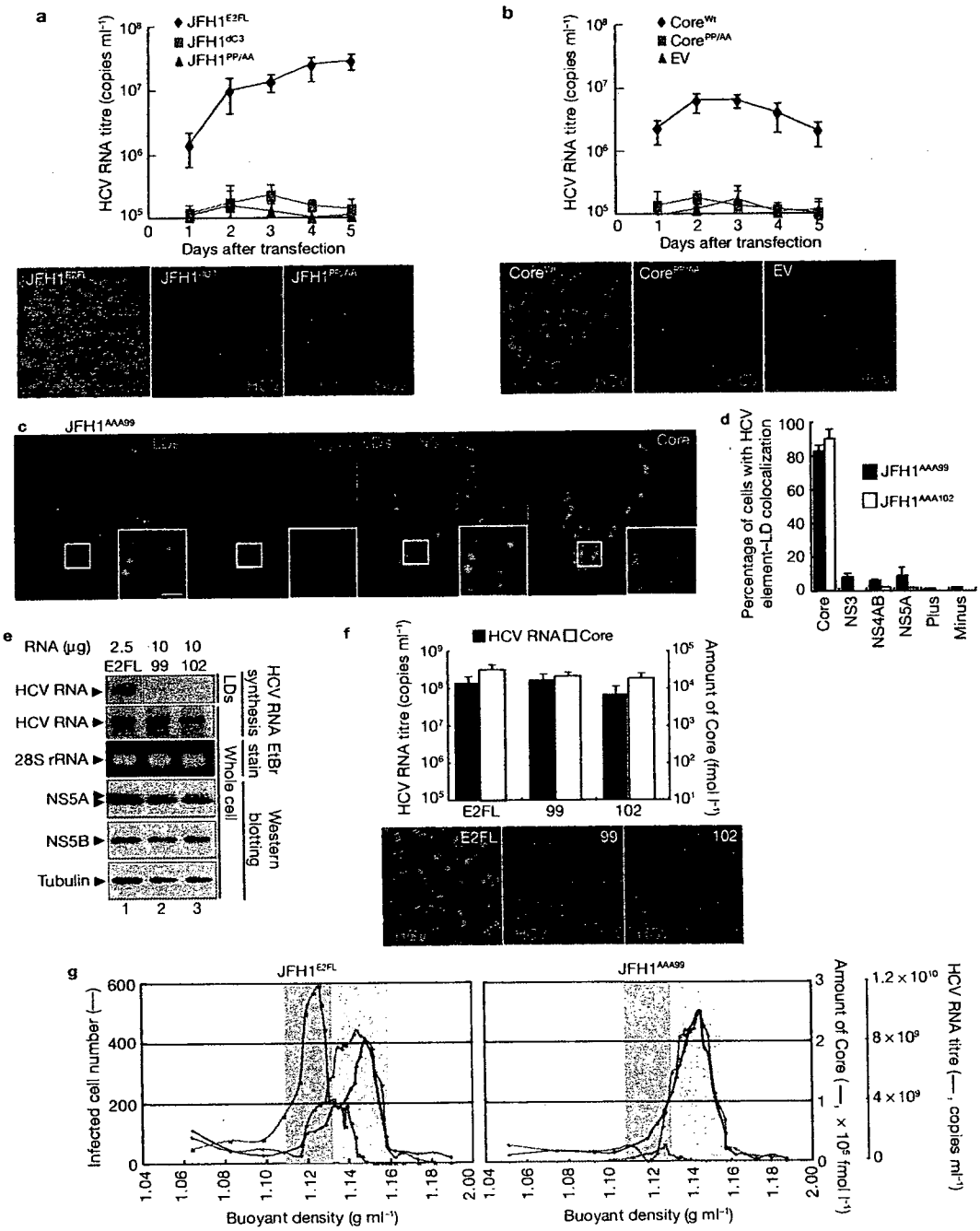

Figure 4 LD associations of Core and NS proteins are necessary for the production of infectious HCV particles. (**a**) The culture medium from JFH1^{E2FL}-, JFH1^{dC3}- or JFH1$^{PP/AA}$-replicating cells was collected at the indicated time points and the titre of hepatitis C virus (HCV) RNA was measured by real-time RT-PCR (upper panel, $n = 3$). The culture medium was added to naïve Huh7.5 cells and, 24 h after inoculation, and cells were labelled with anti-HCV antibodies (lower panels, red). (**b**) JFH1^{dC3} replicon-bearing cells were transfected with pcDNA3 (EV), pcDNA3–Core^{Wt} (Core^{Wt}) or pcDNA3–Core$^{PP/AA}$ (Core$^{PP/AA}$). The level of HCV RNA and the infectivity of the culture medium were examined as described above ($n = 3$). (**c**) Subcellular localization of NS5A and Core in cells expressing JFH1^{AAA99}. The insets are high magnifications of the area of the corresponding panel. Scale bar, 2 μm. (**d**) Percentages of cells in which the signals for given HCV proteins, and plus- and minus-strand HCV RNA, overlapped with those for LDs ($n > 200$). (**e**) Different amounts of JFH1^{E2FL} (E2FL), JFH1^{AAA99} (99) or JFH1^{AAA102} (102) RNAs, respectively, were transfected into the same number of Huh-7 cells. HCV RNA synthesis activity in purified LD fractions (LD) and whole-cell lysates (whole cell) was analysed (HCV RNA synthesis). 28S rRNA was used as a control. Western blot analysis of NS5A, NS5B and tubulin in cells is also shown. All the RNA samples in the top panel were run on the same gel. (**f**) Analysis of HCV released from cells expressing JFH1^{E2FL}, JFH1^{AAA99} or JFH1^{AAA102}. HCV RNA titres (black bars) and amounts of Core (white bars) accumulated in the culture medium at 5 d after RNA transfection were measured (upper panel, $n = 3$). Infectivity of the culture medium for naïve Huh-7.5 cells was analysed as described above (lower panels). (**g**) Concentrated culture medium from JFH1^{E2FL}- and JFH1^{AAA99}-replicating cells was fractionated using 20–50% sucrose density-gradient centrifugation at 100,000 *g* for 16 h. For each fraction, the amounts of Core (black line), HCV RNA (blue line) and infectivity (represented by infected cell numbers in a well; red line) are plotted against the buoyant density (*x*-axis) ($n = 3$). Uncropped images of gels are shown in Supplementary Information Fig. S6. All error bars are derived from s.d.